Application of multi-monitoring methods to investigate the contamination and distributed accumulation of heavy metals at Saphan Hin, Phuket, Thailand

Phuong Khanh Mai

A Thesis Submitted in Fulfillment of the Requirements for the Degree of Master of Science in Earth System Science
Prince of Songkla University
2019

Application of multi-monitoring methods to investigate the contamination and distributed accumulation of heavy metals at Saphan Hin, Phuket, Thailand

Phuong Khanh Mai

A Thesis Submitted in Fulfillment of the Requirements for the Degree of Master of Science in Earth System Science
Prince of Songkla University
2019

Thesis Title	Application of multi-monitoring methods to investigate the contamination and distributed accumulation of heavy metals at Saphan Hin, Phuket, Thailand
Author	Phuong Khanh Mai
Major Program	Earth System Science

Major Advisor

……
(Dr. Avirut Puttiwongrak)

Co-advisor

…….
(Dr. Kritana Prueksakorn**)**

Examining Committee:

……..…Chairperson
(Assoc. Prof. Dr. Pham Huy Giao)

……..…Committee
(Dr. Avirut Puttiwongrak)

……..…Committee
(Dr. Kritana Prueksakorn)

……..…Committee
(Asst. Prof. Thongchai Suteerasak)

……..…Committee
(Dr. Tanwa Arpornthip)

The Graduate School, Prince of Songkla University, has approved this thesis as fulfillment of the requirements for the Master of Science Degree in Earth System Science

……
(Prof. Dr. Damrongsak Faroongsarng)
Dean of Graduate School

This is to certify that the work here submitted is the result of the candidate's own investigations. Due acknowledgment has been made of any assistance received.

.....Signature
(Dr. Avirut Puttiwongrak)
Major Advisor

.....Signature
(Ms. Phuong Khanh Mai)
Candidate

I hereby certify that this work has not been accepted in substance for any degree, and is not being currently submitted in candidature for any degree.

.....Signature

(Ms. Phuong Khanh Mai)

Candidate

Thesis Title Application of multi-monitoring methods to investigate the contamination and distributed accumulation of heavy metals at Saphan Hin, Phuket, Thailand

Author Ms. Phuong Khanh Mai

Major Program Earth System Science

Academic Year 2018

ABSTRACT

Heavy metals have been frequently investigated exceeding the safe threshold in some areas including coastal site, the crucial aquatic source of human food as well as the mining site. In addition, a detail examination for determining the contamination in those areas cost expensively in order to initiate the proper mitigation. This research illustrates the achievement by employing the effective methods such as chemical analysis (CA) utilizing aqua-regia and geo-electrical method including electrical resistivity imaging (ERI) and induced polarization (IP) for estimating the contaminated level in subsurface sediment in an efficient way. The study was done at coastal area, Saphan Hin, Phuket, Thailand situated downstream of Bang-Yai canal which is considered the main pathway bringing heavy metal from the mining industry where the nearest is far about 4 km away. Phuket Island is considered to be one of the most attractive places for tourism in Thailand while Saphan Hin can be seen as the main region for sea fishery to supply the amount of food demand for a large number of tourists coming to visit this Island. The results depict that the exceeding level of possible contamination is at least up to 3 km far from the estuary with the depth in the range from 50 m to 50 cm, requiring the measures for the health of local and tourist people.

Keywords: Coastal Island, Heavy metal contamination, Aqua-regia, Electrical resistivity Imaging, Induced polarization

ACKNOWLEDGMENT

I would like to thank, first and foremost, my main advisor Dr. Avirut Puttiwongrak for guiding and advising me every step of the research process. Without his guidance and immense help, this dissertation would not have been finished.

I would like to express the appreciation to Dr. Kritana Prueksakorn as the co-advisor of this thesis. I am appreciated for his comments on this thesis.

I would like to give my deepest thankfulness to my committee members: Assoc. Prof. Dr. Pham Huy Giao, Asst. Prof. Thongchai Suteerasak, Dr. Tanwa Arpornthip for their encouragement, insightful comments, and useful questions.

I am indebted to Prince of Songkla University (Phuket Campus) and the Interdisciplinary Graduate School of Earth System Science and Andaman Natural Disaster Management (ESSAND) for giving me the study and research opportunities through TECH_AC scholarship.

Beside my adviser and my committee, I sincerely thank all ESSAND teachers, who concerned and encouraged me in the past years.

Also, I thank my friends, my classmates in ESSAND faculty for motivating and helping me the valuable discussions of research.

Last but not least, I wish to thank my family for giving birth to me and supporting me spiritually throughout my life. I might not complete this program without their stand by.

Phuong Khanh Mai

CONTENTS

CONTENTS (Continued)

LIST OF FIGURES

LIST OF FIGURES (Continued)

LIST OF FIGURES (Continued)

LIST OF TABLES

LIST OF ABBREVIATIONS

As	Arsenic
2D	Two Dimensional
3D	Three Dimensional
Ag	Silver
As	Arsenic
Be	Beryllium
CA	Chemical analysis
Cd	Cadmium
CF	Contamination factor
cm	Centimeter
Co	Cobalt
Cr	Chromium
Cu	Copper
DNA	DeoxyriboNucleic Acid
EF	Enrichment Factor
ERI	Electrical resistivity imaging
ERT	Electrical resistivity tomography
Fe	Iron
Hg	Mercury
I	Current
ICP-AES	Perkins-Elmer Optima 3000XL
ICP-OES	Inductively Coupled Plasma Optical Emission Spectrometry
Igeo	Geoaccumulation Index
IP	Induced polarization
m	Meter
MASL	Meters above sea level
mg/kg	Milligram/kilogram
Mn	Manganese

LIST OF ABBREVIATIONS (Continued)

ms	Millisecond
Na	Natri
Ni	Nickel
Ohm-m	Ohmmeter
Pb	Lead
PLI	Pollution load index
R	Correlation Coefficient
Sb	Antimony
Se	Selenium
Sn	Tin
SQGs	Sediment quality guidelines
Sr	Strontium
TDIP	Time domain induced polarization
Ti	Thallium
USA	United State
V	Voltage
Zn	Zinc

CHAPTER 1
INTRODUCTION

1.1 Background of study

Heavy metals is a collective group, including metal and metalloid elements which has atomic density is heavier than 4g/cm3, for instance Lead (Pb), Copper (Cu) and Zinc (Zn), Arsenic (As), Cadmium (Cd), Chromium (Cr), Mercury (Hg), (Edelstein and Ben-Hur 2018). Heavy metal is strongly toxic for livings (Freije 2015) through spoiling DNA and preventing growth (Kennish 1996). Toxicity of heavy metal might reduce fertility, devastating organs and even lead to deaths in animals (Authman 2015). The sort of metal and animal species play an important role in the toxic level of organisms. Normally, the heavy metal existing cannot totally be removed and detoxified (Sharifuzzaman et al. 2016). Pregnant women and offspring are easy to be affected by those toxicants (Neeti and Prakash 2013). Otherwise, because of a long persistence of heavy metal in the environment (Rajeswari and Sailaja 2014), therefore, bioaccumulation and biomagnification through the aquatic food chain will become more serious issues for top predate and human health. A few previous researchers indicated that estuaries are areas that the accumulated amount of heavy metal elements higher than 90% after a long their transportation (Sharifuzzaman et al. 2016). In some sediment, the concentration of heavy metal sometimes is found 100 times higher than those in ambiance (Temara et al. 1998). Hence, sediment is seemed to be a significant element with the presence of metal and pollution in the coastal area (Sharifuzzaman et al. 2016). The contaminated metal might be caused by some chemical and physical factors (Bernard et al. 1997). While physical factor as weathering of rock (González-Acevedo et al. 2018), human activity is normally a principal source, example agriculture activities, disposal of industrial wastes, and mining operation and so on (Salah et al. 2012; Ganugapenta et al. 2018). The heavy metal investigation in sediment was a concerning issue at many counties as India (Harikrishnan et al. 2018), China (Wu et al. 2018), Iran (Ghanbarpour et al. 2013), Poland, England, and Persian Gulf (Helali et al. 2016). In particularly mining

activities almost cause the heavy metal contamination with metal concentration exceeds standard value like tin (Sn) pollution in China (Xiang-bin et al. 2015), Thailand (Suteerasak and Akkajit 2018) or serious pollution from bauxite mining in Malaysia (Kusin et al. 2018).

1.2 Statement of problem

Phuket is located in the southern of Thailand with an area approximately 54 km^2 (Lverson 2017). Before becoming a tourist destination of the world, the main manufacturer of Phuket is tin mines exploitation, this activity brought for Phuket a huge economic resource. In 1995, the final mine closed because of government policy in protecting the environment (Sakunboonpanich 2011). Tin mining operations had been exploiting for hundreds of years, hence, the investigation heavy metal was applied in the subsurface, sediments, water resources at some areas in Phuket (Suteerasak and Bhongsuwan 2006), especially the coastal zones such as Saphan Hin (Suteerasak and Akkajit 2018) and along Bang-Yai canal. Kathu waterfall provides the water for Bang-Yai canal, this canal through abandoned tin mining areas (Kathu; Muaeng districts) and then into Saphan Hin. According to the collected document, heavy metal is many times higher than the standard, especially is Tin (Akkajit et al. 2017). Toward another element as Pb, Zn and Cu were assessed as coexist in sediment at the vicinity of mining areas and along Bangyai canal (Suteerasak and Bhongsuwan 2008). People live in Saphan Hin have been facing to the heavy metal contamination situation, many hypotheses were given as “which is the main source of contamination? Which is the level of contamination? Or how many areas are affected by this pollution?” Until now, however, there are not sui and appropriate answers to be found and these issues are not improved and surmounted. The most popular methods are used to assess the heavy metal contaminations are chemical analysis (CA), magnetic susceptibility or Geo-electrical surveys. Every method has strong and weak points such as the chemical analysis using aqua-regia has high accurate result (Kusin et al. 2018) but its cost is high and locations, chemical types for detection must be carefully set and it might not be sufficient to cover all suspected areas for some time (Akkajit et al. 2017). The magnetic indicator has been

frequently applied for the measurement of heavy metals due to its principles for a correlation between the intensity of heavy metals and susceptibility of magnetic (Ravisankar et al. 2017). However, magnetic does adapt to all metals and metalloids, not all the time (Rachwał et al. 2017). Hence, combining multiple methods to assess heavy metal pollution is necessary. In this study, chemical analysis method and electrical resistivity will be connected together to investigate soil contamination, determine the extent of the contamination zone and assess heavy metal concentration in the study area also.

1.3 Research objective

1. To assess the contaminated level heavy metal in topsoil at coastal Saphan Hin by Geo-chemical method
2. To determine the extent, distribution, and source of the heavy metal pollution by combination Resistivity and Induced Polarization imagine
3. To establish a correlation between resistivity value and the concentration of heavy metal

1.4 Scope

+ Area: This research is implemented at Saphan Hin coastal area and a part along Bang Yai canal, in Wichit, Mueang District, Phuket Island, Thailand.
+ Method: Using geo-electrical surveys for investigating subsoil contamination, particularly ERI and IP are conducted in the study area.

  Applying geochemical analysis to determine the contaminated concentration at the sampling points.
+ Time: This research will be conducted in two years. From August 2017 to May 2018 identifying the risk areas, finding research material and methods have done. Continuously, the field survey (electrical resistivity survey and collecting sample) and chemical validation

will operate from June 2017 to April 2019. Finally, the full thesis will be completed before June 2019 to send to the authoritative committee to be valued.

CHAPTER 2
LITERATURE REVIEW

2.1 Heavy metal

Heavy metal is defined as metallic chemical factors that often are high density and although at low concentrations, it has an amount of poisonous (Neeti and Prakash 2013). In the periodic , there are 118 chemical elements, heavy metal is a group with 19 elements (such as arsenic (As), Manganese (Mg); Chromium (Cr); Copper (Cu); Zinc (Zn); Iron (Fe); Cobalt (Co); Tin (Sn); Gold (Au); Lead (Pb); Nickel (Ni); Gallium (Ga); Germanium (Ge); Zirconium (Zr); Niobium (Nb); Silver (Ag); Cadmium (Cd); Mercury (Hg) so on), which have many commonality about chemical and physical properties and outstandingly different from the remaining 97 known elements. Lead, cadmium, and mercury do not only seem to be non-beneficial and insignificant toward biology but also extremely toxic. When heavy metal is dispersed in the biosphere, it is difficult to recover or reduce them. Therefore, the environmental harmful effects of these metals are permanent, especially with chromium, copper, manganese nickel, tin, and zinc (Rajeswari and Sailaja 2014). Currently, heavy metal contamination is considered a principal environment issue since the ions of metal accumulates in the natural environment because they are non-degradable elements (Ganugapenta et al. 2018). The tendency of either bioaccumulation or toxicity of those heavy metals can harm living organisms' health. Because heavy metals are not able to be broken down through either biological or chemical processes; therefore, their concentration only reduces by transformation or movement in space. Heavy metals are naturally occurring in the forms which are incompletely available for absorbing by vegetation (Sharifuzzaman et al. 2016). Fundamentally, they are insoluble forms such as mineral structures, precipitated or chemical compound that is very hard for plant to absorb in soil. Comparing with anthropogenic activity source, the heavy metal accumulation in crust is relatively high. The presence of heavy metal in the environment is often made by a few natural processes as weathering, erosion, volcanic, eruptions and comets. On the other hand, anthropogenic sources predominantly the heavy metal contamination in soil, water,

air: alloy production, mining operations, battery production, deposition of atmospheric, bio-solids, explosive producing, incorrect way in stacking and treating industrial solid waste, leather manufacture, fertilizer and pesticide fabrication, pigments, printing ink, printing power, photographic materials, sewage irrigation, wood preservation, clothing industry (textiles, dyes), electronic industries, and metallurgical industry (smelting, steel…) (Rajeswari and Sailaja 2014). Source of heavy metal, properties of soil, level of concentration of heavy metal in soil, the degree and extent of uptake by plants or animal affect are factors, affected to concentration of heavy metal in food process. If the heavy metals concentration in geochemical process is higher than permission standard, it might be harmful and toxic to all species. Generally, both the weathering of parent materials, and the alteration of the anthropogenic geochemical cycle released for the environment high metal waste. These activities cause the negative impact in the environment, for instance, losing of biodiversity, changing or destructing the ecosystem or environment pollution. In particular, mining activities are mentioned be the predominant polluted source of heavy metals in the sediment. The recovery of ecosystems from any kind of mining exploitations might be a long-last process because exploiting mines caused large quantities of stockpile without treatment frequently. By the time, abandoned mines cause directly contamination of aquifer through chemical run-off or leachate destroyed heavily environment. In conclusion, treating heavy metal accumulation is imperative in every manufacturer.

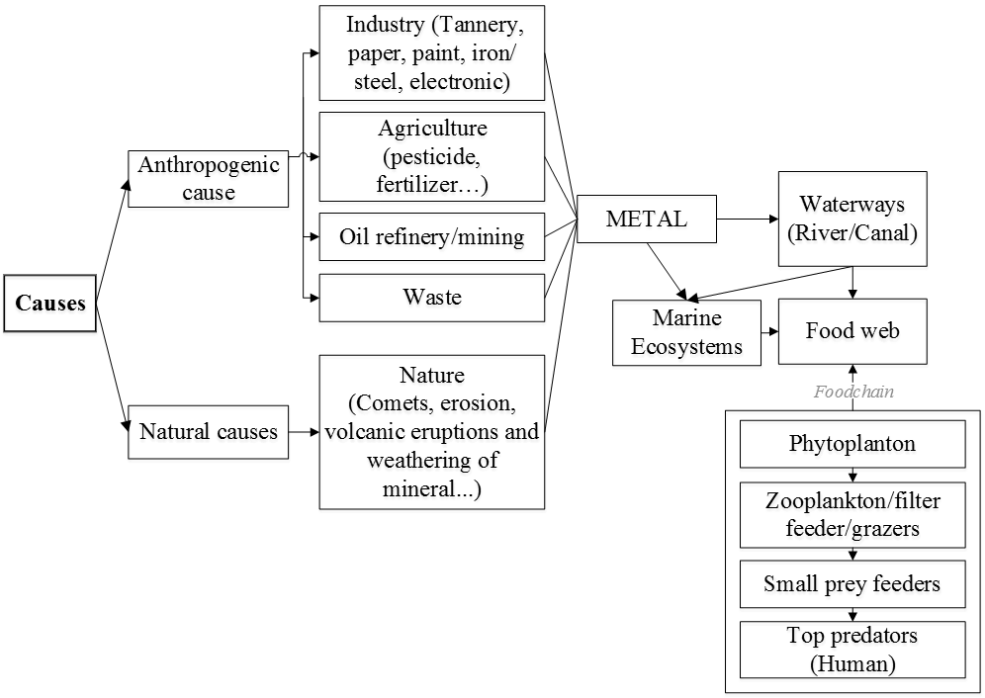

Figure 2.1 Causes and transformation of heavy metal in nature, modified from (Sharifuzzaman et al. 2016)

Sources, the effect of heavy metal toward people, plant and microorganisms are briefly illustrated in table below.

Table 2.1 Effect of heavy metal toward people, plant and microorganisms (Ayangbenro and Babalola 2017)

Contaminants	Source	Effects		
		Human	**Plant**	**Microorganism**
Antimony (Sb)	Coal burning, mining, smelting, volcanic eruption, soil erosion.	Cancer, liver, cardiovascular problems, conjunctiva of the eyes, dermatitis, nasal ulceration, diseases of the respiratory system	Reduced synthesis process of metabolites, inhibit growth, chlorophyll synthesis inhabitation Reduced synthesis process of metabolites, inhibit growth, chlorophyll synthesis inhabitation	Curb activities of enzyme, growth rate increase
Arsenic (As)	Atmospheric deposition, pesticides, mining, smelting, sedimentation in earth crust	Hurt and destroy brain, cardiovascular and respiratory disease, conjunctivitis, and skin cancer	Destroy cell membrane, inhibit growth, inhibit roots elongation and proliferation, hampers with metabolic processes, increase sterility, physiological disorders and	Deactivate enzymes activities

Contaminants	Source	Effects		
		Human	**Plant**	**Microorganism**
			reduce the productivity of fruit and yield	
Beryllium (Be)	Coal and oil burning, dust of volcanic	Allergic reactions, lung and heart diseases, cancer	Inhibit the germination process of seed	Lead to chromosomal aberration, mutation issues
Cadmium (Cd)	Fertilizer, pesticide, plastic, mining (exploiting, refining), electric welding	Bone disease, respiratory disease (coughing, emphysema of lung), vomiting, headache, hypertension, kidney diseases, prostate cancer, lymphocytosis, anemia, inhabit human fertility	Reduce nutrient content in plant, growth inhibition, chlorosis, inhibit the germination process of seed	Damage nucleic acid, change protein, prevent cell division and cell transcript, and inhibit carbon and nitrogen mineralization
Chromium (Cr)	Dyeing, metal plating, paints fabrication, steel production, textile industry, leather tanning, pigment or dyeing	Bronchopneumonia , diarrhea, headache, allergy of the skin, itching, liver and respiratory diseases, lung cancer, vomiting, sickness, inhabit renal, harmful for reproductive organs.	Chlorosis, detain and wilting the growth of plant, biochemical lesions, reduced biosynthesis germination, cause the shortage of oxygen.	Growth inhibition, oxygen uptake inhibition, depth

Contaminants	Source	Effects		
		Human	**Plant**	**Microorganism**
Copper (Cu)	Copper burnishing, mining operations, paints fabrication, plating, printing fabrication	Abdominal hurt, diarrhea, anemia, headache, destroy liver and kidney, metabolic disarray	Chlorosis, cause the shortage of oxygen, inhibit growth	Interrupt cellular function, and conquer enzyme activities
Mercury (Hg)	Batteries, coal burning, geothermal activities, mining operations, paints fabrication, paper manufacture, natural activities (volcanic eruption, weathering of rocks)	Ataxia, lost concentration, blindness, deafness, reduce rate of fertility, dementia, dizziness, dam, gastrointestinal hurt, gingivitis, kidney and lung disease, sclerosis, loss of memory, reduced immunity	Affects ant oxidative system, photosynthesis influence, enhance lipid peroxidation, reduce the genotoxic effect, curb growth, nutrient of plant, yield, and shortage of oxygen	Decline population size, denature protein, disturb cell membrane, conquer function of the enzyme
Lead (Pb)	Coal burning, electroplating, batteries industry, mining operation, paints	Anorexia, damage to neurons, high blood pressure, hyperactivity, sleeplessness, lost concentration, reduced fertility,	Disturbs photosynthesis and growth, chlorosis, prevent enzyme activities and	Change and denatures nucleic acid and protein, prevent enzymes activities and transcription

Contaminants	Source	Effects		
		Human	Plant	Microorganism
Lead (Pb)	fabrication, pigments, dyes	damage renal system, a risk factor for Alzheimer's disease, kidney diseases	inhibit seed germination, shortage oxygen	
Nickel (Ni)	Electroplating, coal burning, non-ferrous metal, paints, porcelain enameling, trash incinerator	Cardiovascular diseases, nickel allergy, chest pain, dermatitis, dizziness, vomiting, respiratory disease (dry cough, shortness of breath), headache, kidney, lung diseases, cancer,	Reduction chlorophyll content, prevent enzyme activities and growth, reduced nutrient consumption	Disturb cell membrane, prevent enzyme activities, shortage of oxygen
Selenium (Se)	Coal burning, mining operations	Disturb the endocrine system, stomachache, destroy cells activity, liver damage	Adjustment of protein properties, decrease of plant biomass	Prevent the growth rate
Silver (Ag)	Battery production, mining operation, photographic processing, smelting	Respiratory diseases, pharynx problems, and chest hurt, rheumatism, poisoning, depth	Disturbs homeostasis, reduce chlorophyll, conquer growth	Destroy and inhibit transduction and growth of cell

Contaminants	Source	Effects		
		Human	Plant	Microorganism
Titanium (Ti)	Cement fabrication, fossil fuels burning, metal smelting, oil refining, pesticide	Hair fall, ataxia, coma, convulsions, dizziness, vomiting, headache, tired, gastroenteritis, hallucinations, hypotension, sleeplessness, tachycardia	Prevent enzyme activities, reduced growth	Damages DNA, prevent enzyme activities and growth of microorganism
Zinc (Zn)	Brass industry, mining operations, oil refinery, plumbing production,	Ataxia, gastrointestinal hurt, icterus, impotence at male, destroy muscle, kidney and liver, lethargy, fever, vomiting, headache, tired, cancer, depth	photosynthesis effect, prevent growth rate, decrease chlorophyll content, inhibit germination rate and plant biomass	Decrease biomass, conquer growth, death
Tin (Sn)	Food product manufacture, mining.	Tin (II) can irritate to human skin, eyes cause vomiting, headaches, sickness, dizziness and urination problem. With long-term effects, they can cause depressions, liver	Inhibit growth, reproduction, disturbing enzymatic systems, and aquatic organisms and plant system.	Toxic to fungi, algae, and phytoplankton.

Contaminants	Source	Effects		
		Human	Plant	Microorganism
Tin ***(Sn)***		damage, shortage of red blood cells and brain damage and so on.		

2.2 Accumulation of heavy metal contamination in groundwater and sediment

Sediment is any particulate composition that can be moved by fluid flow and which finally is gathered as a layer of solid atoms on the bed or bottom of a mass of water or other liquid (National Geogrphic 2019). Sediments are a combination of various components of mineral types as organic trash, characterize as an eventual sink for heavy metals released into the environment (Salah et al. 2012). Recently, the previous research had shown that river sediments and coastal sediments, in turn, are area have highest contamination of heavy metals (Sharifuzzaman et al. 2016; Ganugapenta et al. 2018), sediment from coastal surroundings near industrial and metropolitan regions are fundamentally contaminated to the amount of heavy metals, which are poisonous to biota (Satpathy et al. 2011). As a result of either diagenesis and physical disturbance, metals accumulation can be afterward discharged to the overlying water column and existed a long time after stopping the direct release. Furthermore, the interaction of redox changes, the affecting metal concentrations between water and heavy metal play an important role in the effect of the sediment-water interface (Santschi et al. 1990). This process will continuously transfer into the water and make degradation toward water quality (Salah et al. 2012). Nowadays, industrialization-modernization and anthropogenic activities have been creating heavy metal pollution in many countries. USA, European Union, Australia, China spearheaded the numerous pollution sites. For instance, at United State, having more than1000000 sites, in European Union with more than 80000 sites, Australia with about 50000 places and in China, only Asian country, there are approximately 1.0 million km^2 (Xiang-bin et al. 2015). Remarkably, it is the heavy metal accumulation at estuarial and coastal zone such as Tupilipalem Coast, southeast coast of Indian (Ganugapenta et al. 2018); Kalpakkam, East Coast of India (Satpathy et al. 2011); The Canakkale strait (Dardanelles), between Marmara Sea and Aegean Sea, Turkey (Ilgar and Sari 2008); Semarang rivers, Indonesia (Nurbaiti. 2011); the Turag river in Bangladesh (Mohiuddin et al. 2016); Masinga Reservoir, Kenya (Nzeve et al. 2014); Xijiu Lake, Taihu Lake Catchment, China (Bing et al. 2011).

Mining exploiting and anthropogenic activities cause the concentration of elements in narrow space, for instance, ore area or a landfill, waste site (Gautam et

al. 2016). The heavy mental existence of anomalous accumulation doesn't stay s forever particular in the weathering environment. The dispersion of concentration element may lead to the spatial patterns for around area, this phenomenon is called as aureoles or halos. These aureoles often have bigger in size than the original zone, and lower at concentration than normal background concentration values (de Smeth 2005). However, the change of condition effects to this element dispersion. Normally, temperature, gas, pressures are factors leading to a metamorphic phase, but almost the dispersion processes are triggered by the influence of oxygen, carbon dioxide, water, temperature, mechanical forces (secondary dispersion). The level of dispersion depends on the factor toward every heavy metal element.

Table 2.2 The factors affect the level of heavy metal dispersion

Secondary dispersion	**Transport mechanism**	**Transport distance from source**
Mechanical - clastic	Gravity, win, water, ice	Capable of many km
Chemical - hydromorphic	Laterally by groundwater movement Vertically by capillary ascent	Up to two km Vertically
Gaseous	Advection and diffusion	Approximately several hundred meters
Organic Processes	Plant uptake from depth Bioturbation	Around tens of meters.
Electrochemically induced	Redox potential differences	Horizontally limited Vertically about 100m

The dispersion and accumulation of heavy metal are described in the picture below.

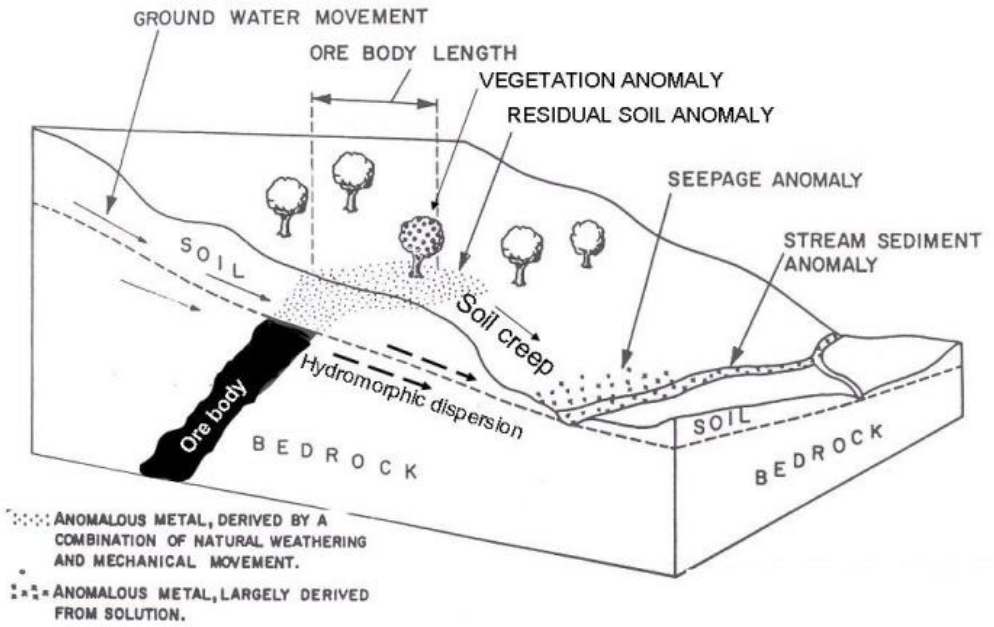

Figure 2.2 Simplified model showing the formation of geochemical anomalies in a the situation was the bedrock is covered by residual soil (de Smeth 2005)

In nature, when there are effect of external factors (raining, wind, erosion…) and internal factors (gravity, groundwater…) the heavy metal dispersion at the ore area was destroyed and then moved and created the disposition at coastal or sediment of stream, river through the relative variety process including few steps. The catalysis of water from rain or soil gravity makes the hydromorphic dispersion, then the heavy metal molecules will transport follow the groundwater zone from high elevation to low elevation in terrain and after that forming seepage anomaly and stream sediment anomaly. It is the reasons to support that estuarial areas always exist a number of heavy metal elements.

2.3 Contaminated source from Tin mining

The abandoned mine is deemed containing a huge deposition of mining waste (i.e. tailings) in a man-made lake, the locations have steep and rough topography (Yaacob et al. 2009). Contamination of abandoned mines is a quite characterized and local phenomenon, however, its effect on environment and human is very spectacular (National Rivers Authority 1994). In the mining industry, heavy

mental at wasteland is hot environmental problem and tin mining pollution is also a similar issue (Xiang-bin et al. 2015). Tin is found naturally in the Earth's crust, with a medium concentration of nearly 2-3 mg/kg (Budavari 2001).In nature, Tin is a metal with grey-white cover, the most popular and significant inorganics of tin are the tin II ($Sn^{2+)}$ and tin IV chlorides ($SnCl_4$), tin II oxide (SnO_2), tin II fluoride (SnF_2). Moreover, the Sn^{2+} and Sn^{4+} oxidation states of tin are two partially s elements. Compounds of tin are diverse in the environment from inorganic to the organic structure. Tin release to the environment through many activities including natural and anthropogenic process e.g: exploiting, smelting and refining tin (Organization 2005). There are the amount of compositions and applications of tin alloys. Tin alloys contain a large of compositions and many applications. A numerous number of tin alloys always keep lead, antimony, silver, zinc, or indium. China, Indonesia, Peru, Bolivia, Brazil, Australia, especially Thailand, Malaysia are countries, having the in-producing field is the biggest in the world. In life, tin has much useful application as protecting coating for other metals (food containers); decreasing the organic and inorganic synthesis in producing metalized glazing or glass (Organization 2005). Tin is often found as cassiterite (SnO_2), beside it exists with varied forms, example: teallite ($PbSnS_2$), canfieldite (Ag_8SnS_6), cylindrite ($PbSn_4FeSb_2S_{14}$), and stannite (Cu_2FeSnS_4) (Beliles 1994). Tin and tin alloy exist in all types of environment like water, water, soil, and sediment but in water, tin compound is broadly only sparingly soluble and then separation to soils and sediments. Tin in water will not volatilize or transform into aeriform (Cooney 1988), however, it can transfer from water, soil, sediment to plant system with coefficients from 0.01 to 0.1 (Kloke et al. 1984). At Phuket, range of tin value in ppm was found in many rock types, for instance in sediment (0-30 ppm), Adamellites (0-70 ppm), Granite at central of Phuket island (40-10000 ppm), Granite at Khao Muaeng (5-2000 ppm) (Garson et al 1975).

2.4 Geo-electrical methods

Heavy metal is the hot issue on the world, therefore numerous methods were researched and applied for assessing and finding out the contamination such as geo-electrical resistivity; chemical analyzing (by calculating pollution load index

(PLI); contamination factor (CF) values (Saraee et al. 2011) or statistic method. Nevertheless, methods are largely applied and be the most popular are geo-electrical and chemical analyzing.

The geo-electrical surveys are used to measure and detect the physical properties of the subsurface as the position of water and quality of water, water instrument, the structure of soil, characteristic of soil (acidity, contamination, and an anomaly). Electrical resistivity tomography (ERT), also called as electrical resistivity imaging (ERI) (Rehman et al. 2016), is the most popular method in a geophysical techniques (González et al. 2016) for estimating structure of sub-surface by electrical resistivity measurements, which set up on the surface or through using electrodes in one or boreholes. The sites of electrode affect to the depth of information result: In the boreholes, deeper electrodes are suspended; more data of sections can be explored. In ERI method, the received information might be shown both the vertical and the lateral direction. The applied different electrode conformation in ERI has confirmed that this is an effective method in demonstrate resistivity anomalies in near surface with high resolution and used in large environment issues, for instance water content, structure of lithology (González et al. 2016), detecting pollutants (Grellier et al. 2004) or finding ionic impurities in groundwater because of resistivity contrary between contaminated area and rocks (Mathizhagan et al. 2012). The combination profiling and sounding electrical resistivity method was created electrical imaging of near-surface materials. Electrodes were constructed by stainless steel every electrode is around 50 cm length and 2cm diameter. Electrode has duty to inject electrical current with ground. In case, grounding is dry, water need be added to increase the inducting of electrical current because the interaction between electrodes and soil affect to the penetration of current (Rehman et al. 2016). Rising the interval electrode space is one way to the deeper information.

2.4.1 Electrical Resistivity

The resistivity is calculated through measuring induced current and the potential difference, which is directed to as “apparent resistivity” (Anomohanran 2018). This method has been applying for 50 years, measuring electrical resistivity value of a material depend on four electrodes: two electrodes (electrode A and B) to

measure electrical current, and another two electrodes (electrode M and N) to measure their potential:

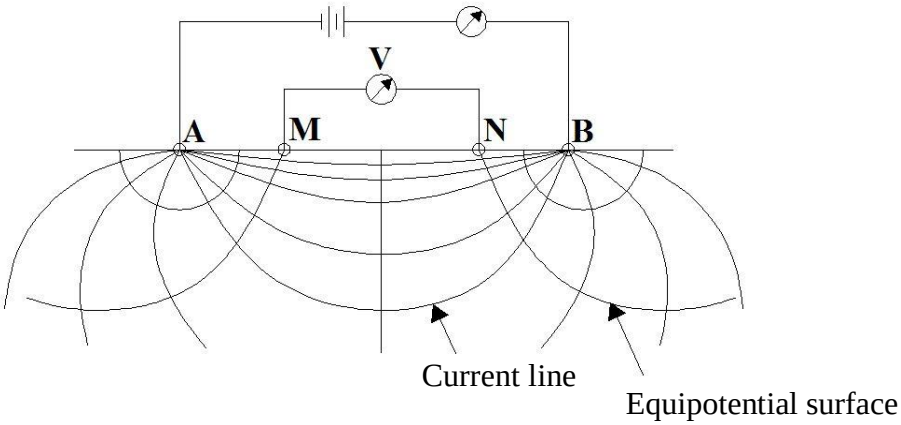

Figure 2.3 General resistivity principal of four electrodes. (Environmental Geophysics 2016)

Base on the understanding difference between electric field potential (ΔV) and the current (I) and distance between the electrodes, the apparent resistivity of the materials can be computed (Koda et al. 2017). The apparent electrical resistivity is established to follow this formula:

$$\rho_a = k \times R \text{ (Koda et al. 2017)} \quad (1)$$

While:

$$R = \frac{\Delta V}{I} \quad (2)$$

$$k = \frac{2\pi}{(\frac{1}{AM} - \frac{1}{BM} - \frac{1}{AN} + \frac{1}{BN})} \quad (3)$$

Where:

ρ_a: apparent resistivity (Ohm.m);

k: geometry factor for used array (m);

R: electrical resistance (Ohm);

I: intensity of current applied to the soil by electrodes AB (mA);

ΔV: different potential between electrodes MN (mV);

$\overline{AM}$, $\overline{BM}$, $\overline{AN}$, $\overline{BN}$: distances between electrodes (m).

However, k value will be adjusted to associate to every case:

a) Wenner array

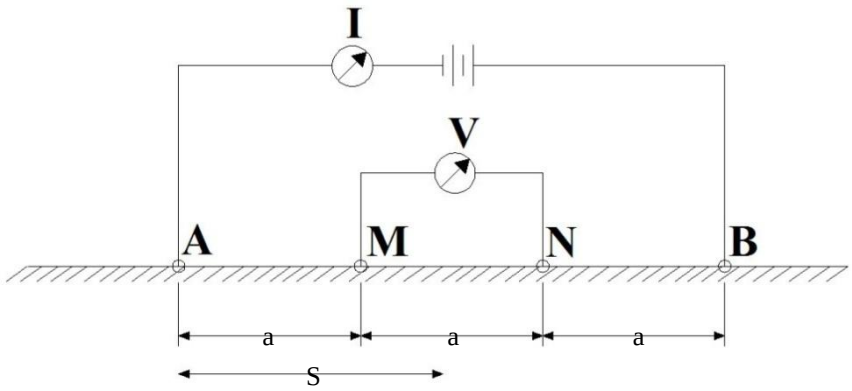

Figure 2.4 Wenner array

$$k = \pi a\left[\left(\frac{s}{a}\right)^2 - \frac{1}{4}\right] \quad (4)$$

$$=> \rho_a = \pi\left[\frac{s^2}{a} - \frac{a}{4}\right] \times \frac{V}{I} = \pi a\left[\left(\frac{s}{a}\right)^2 - \frac{1}{4}\right] \times \frac{\Delta V}{I} \quad (5)$$

Where S is a distance of outer (current electrodes); a is equal intervals.

b) Dipole-dipole Array

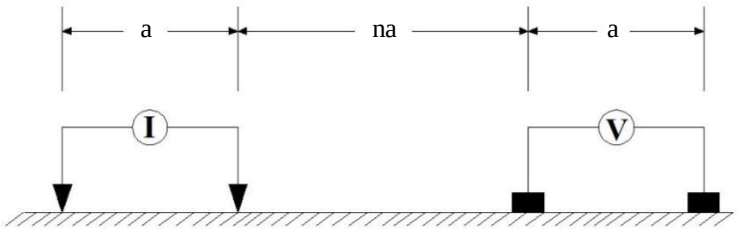

Figure 2.5 Dipole-dipole Array

$$k = \pi an(n+1)(n+2) \quad (6)$$

$$=> \rho_a = \pi an(n+1)(n+2) \times \frac{\Delta V}{I} \quad (7)$$

Where, n= 1,2,3,4…

c) Schlumberger Array

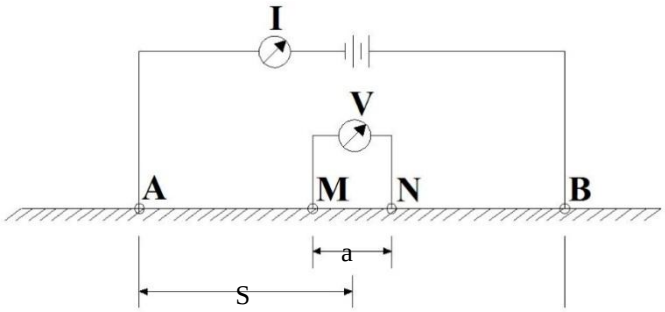

Figure 2.6 Schlumberger Array

$$k = \pi\left[\frac{s^2}{a} - \frac{a}{4}\right] = \pi a\left[\left(\frac{s}{a}\right)^2 - \frac{1}{4}\right] \quad (8)$$

$$\Rightarrow \rho_a = \pi a\left[\left(\frac{s}{a}\right)^2 - \frac{1}{4}\right] \times \frac{\Delta V}{I} \quad (9)$$

2.4.2 Induced polarization (IP)

Induced polarization (IP) is a current-stimulated electrical phenomenon, detected as a delayed voltage reaction in earth materials. An obtained IP is illustrated with a 4 standard electrodes spread. The current abruptly stops, the voltage run along the potential electrodes does not become to 0 immediately but decays slowly reduce to its steady-state value. A popular parameter used to measure IP is chargeability, which is explained as the ratio of the secondary potential over the primary potential of the transfer current. It is applied extensively in the finding mineralization in base-metal and to a slight extent in searching groundwater, ions in rock or metallic ore. Around recent 10 years, IP method has increased application in groundwater and researching environment as seawater intrusion (Martinho et al. 2004), charting lithological layers of unconsolidated sediments or support for interpreting types of ion, which are the result from other geophysical technique (González et al. 2016). The resistivity measurements showed that it is a good tool for mapping composition of the subsurface, however, with the combination of IP value, the effect will be more accurate (González et al. 2016). Adding IP information to traditional resistivity data is very meaningful in ascertaining the type of materials, in particular, IP help the discrimination between clay and sand containing more easily.

Because, these materials are low resistivity value, however, while saline water has high conductivity and low IP; clay has high IP value (Sharma 1997). There are 2 ways to measure IP: making them as a function of time or frequency.

+ Time-Domain IP (TDIP) measure decay voltage as a role of time after switching off current (Guinea et al. 2010).

+ Frequency-Domain IP: Measure apparent resistivity at 2 or bigger than 2, however not over limited 10 Hz.

Time-Domain IP is calculated when a DC current connects with ground, its magnitude is shown as below:

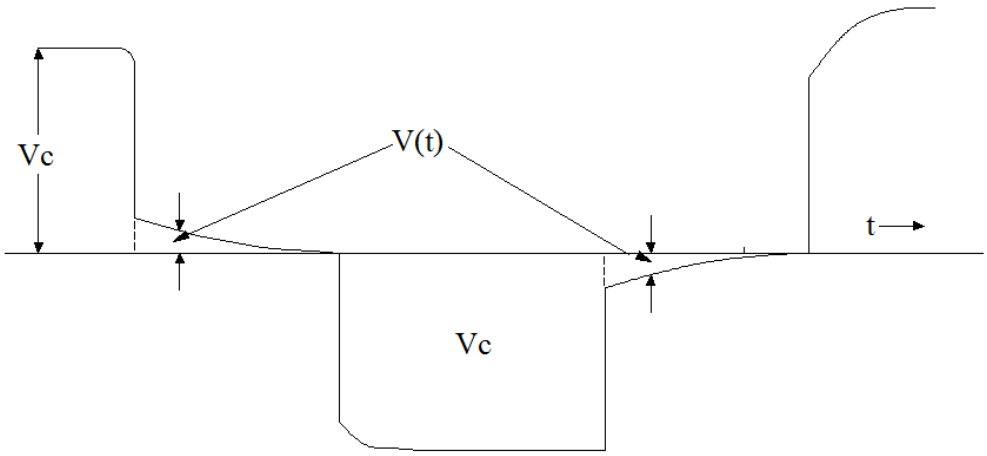

Figure 2.7 Time interval t (from 0.1 to10 s) when turn on and turn off current

$$IP = \frac{V(t)}{Vc} \text{ (mV/V or ms)} \qquad (10)$$

Where, V(t) is a residual voltage (the voltage remains at moment t after the current is switched off); Vc is "primary" voltage (the voltage existed when the current was running; t is time interval (often varied from 1 to 10s when current switch on and off).

* In a clear interval time t from t_a to t_b, IP is defined as:

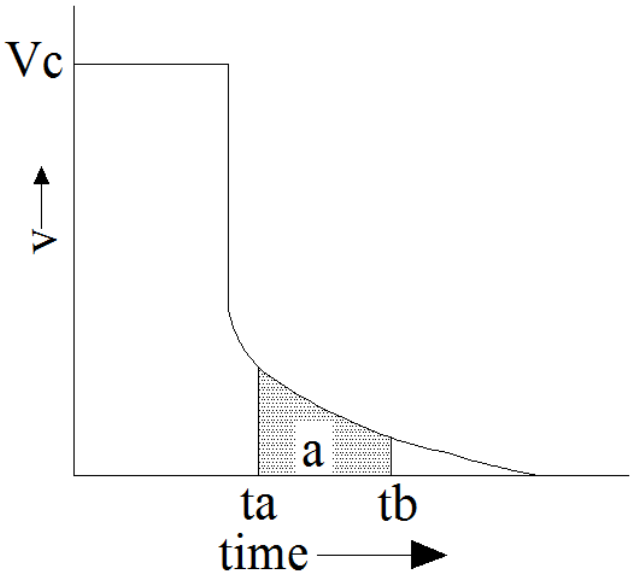

Figure 2.8 Measure of chargeability

$$M = \frac{1}{Vc}\int_{t_b}^{t_a} V(t)dt \quad \text{(Srigutomo et al., 2016)} \qquad (11)$$

Where, M is chargeability (mV/V or ms); Vc is "primary" voltage; t_a,t_b are time may be limited within the off-time, and there are not any standards, so comparing the results between different surveys is difficult; V(t) is residual voltage.

2.5 Heavy metal assessment using Geo-electrical

High heavy metal in contamination plume usually associated with ion concentration and this is the reason made resistivity values become low. Therefore, geo-electrical techniques are a useful tool for indicating contamination zone made from contaminated areas (Ustra et al. 2011). A large literature about applying resistivity imaging techniques to environmental studies has reported such as:

At Nigeria, Abdullahi, N.K and his friends successfully used integrated geophysical techniques with 2D electrical resistivity/ induces polarization imaging in the investigation of groundwater contamination. Time-lapse measurement (in the rainy season and dry season) had been done for four lines of ERI/IP in the dump. The aim of this measurement was proceeded to determine how climate changes or seasonal changes could affect the generation and migration of leachate or

contamination. To detect the structure of subsurface which might impact the leachate outside the boundary of the dump zone, a couple of ERI profiles were done inside boundary of the dump. In terms of running a field survey of ERI/IP, ABEM 4000Terrameter provide with a multi-electrode switch system (42 channels) were utilized. Also, RES2DINV software was used to invert the result of both apparent resistivity and chargeability. It was clear from the inversion result that the low resistivity value and chargeability ranging from 6 – 33 Ohm-m and around 4 msec respectively were interpreted as the leachate plume, while a relatively high IP ranging from 8 to 13 msec were evaluated as clay-rich zones (Abdullahi et al. 2011).

Owing to migration of leachate, landfills are considered the roots of both groundwater and soil pollution; therefore, this research was set up to specify the spatial extent contamination in/ around the dump zone of Seri Petaling, Malaysia. Not only the spatial extent of pollution was determined, but surface water condition locating near the study area was also investigated. The multi-method including geo-electric imaging, groundwater geochemistry and chemical analysis of water samples from two sites of the landfill (upstream and downstream) were carried out. To determine the quality of water, the surface water was used to analyze. Regarding geo-electric imaging, OYO McOhm resistivity meter was used to measure the ground resistance on the top of the landfill with a total length of 250 m in order to get 392 data points. The result clarified that the sites where resistivity value is lower than 10 Ohm, often indicates pollution: Sand saturate with leachate, fresh water (plant materials, rubber strands, sand) saturated with leachate, soil saturated with leachate are respectively 2.994 Ohm, 4.96-5.05 Ohm, 6.03-7.16 Ohm, and 3.51-4 Ohm. The results were confirmed with soil chemical analysis result and the resistivity values obtained from the laboratory measurements for the landfill material and other earth materials at certain localities in Malaysia (Ahmed 2001).

Another research of Martinho, and Almelda using 2D resistivity/IP imaging and then build 3D behavior of contamination in landfill sites in Portugal illustrated the connection between resistivity, IP value, and contaminated plume. ERI/IP measurement was applied to expectedly get the high accuracy of the spatial model. Two Ovar survey combined two profiles using a Wenner standard pseudo-section. In those cases, both negative and positive value can be found simultaneously

enabling to explain predominantly by the influence of 2D or 3D made by the presence of the conductive zones. The resistivity data were inverted by RES2DINV software. Both resistivity and chargeability were demonstrated in pseudo-sections. According to I'lhavo resistivity inversion, a value seemed as the contaminated sand has resistivity value less than around 45 Ohm-m and located at around 4m in depth. Also, the high chargeability value is more than 8 mV/V can be evaluated as well since resistivity value of sand formations is higher than that of mud.

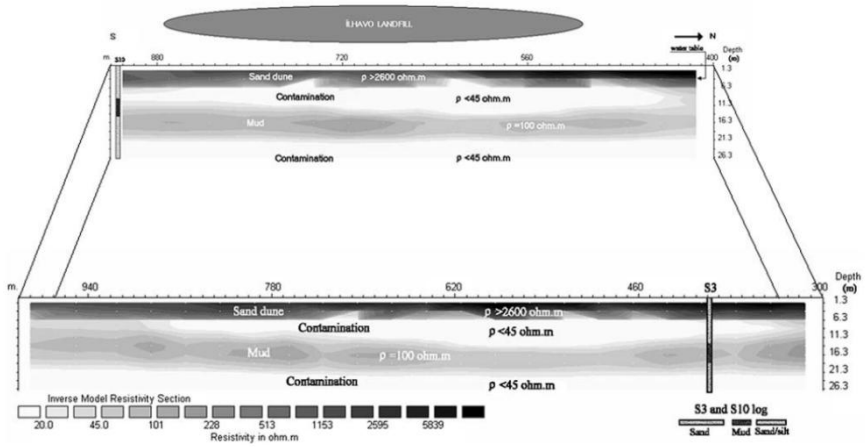

Figure 2.9 Contaminated areas determination through resistivity model for the Ovar landfill

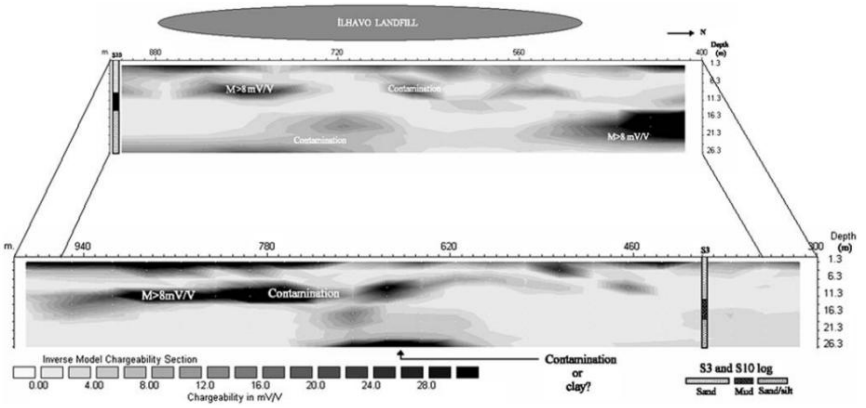

Figure 2.10 Chargeability imaging for the Ovar landfill

In 2016, at Nelfort, Bichet et al used electrical resistivity tomography to detect spatial characterization of leachate plume in a landfill of old and new cells France Bichet. From 1976 to 2002, the Etueffont landfill worked to solve the domestic waste problem of around 47,650 populations. The site combined two parts:

(From 1976 to 1999) the original landfill site (named the old landfill (OL); a newer section named as the new cell (NC) (between 1999 and 2002). With 21 electrical profile lines, the author's group was found the extension of leachate plume from the old landfill and to the productivity of the liner of the NC during dry seasons between 2009 and 2011.

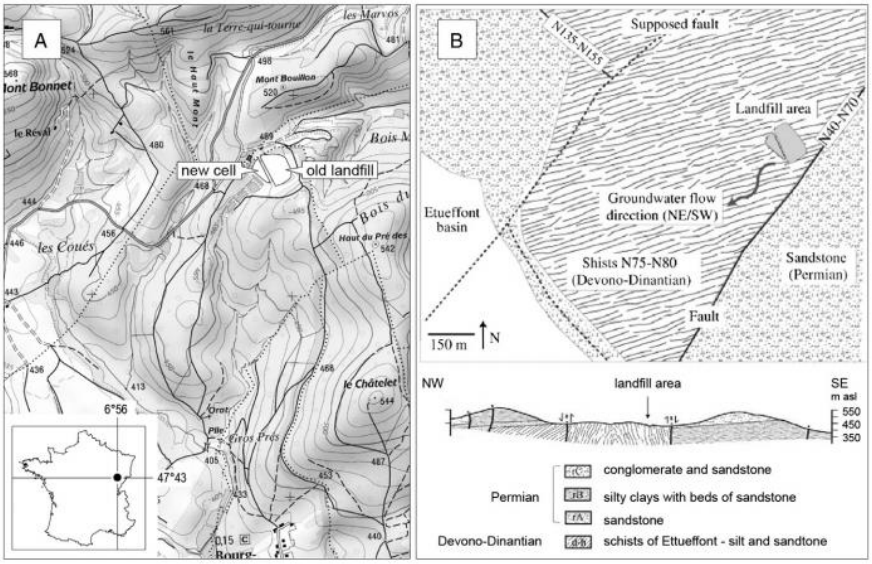

Figure 2.11 Place of the Etueffont landfill: the old landfill (OL) and the new cell (NC)

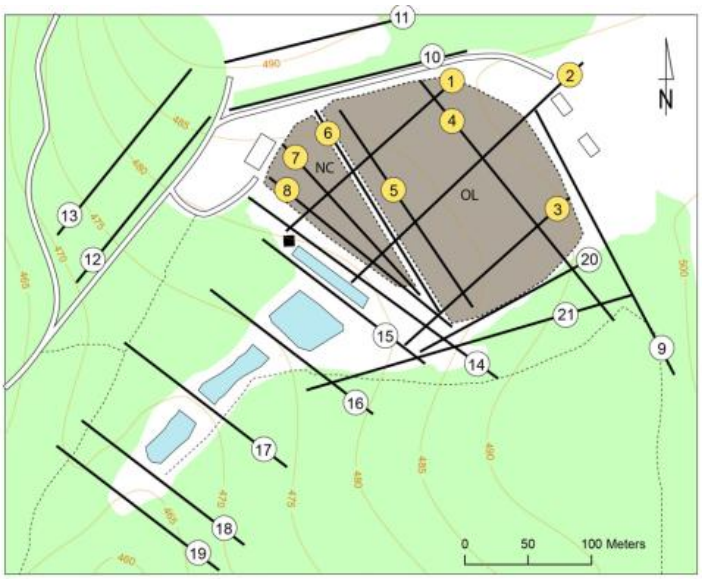

Figure 2.12 Twenty-one electrical profile lines Electrical profiles (black lines)

The inverted results of each profile indicate the contrast of materials. The conductive zone can be seen in the areas fluctuating from dark to light blue with

almost the resistivity value lower than 20 Ohm-m, while the poor conductive zones with the resistivity greater than 300 Ohm-m were depicted in red to brown areas. Hence, 2D geo-electric imaging is very useful to detect the spatial extent of pollution and also to determine the leachate bio-stabilization ranging from 10 to 50 Ohm-m (Bichet et al. 2016). A few contaminated plumes are shown below images:

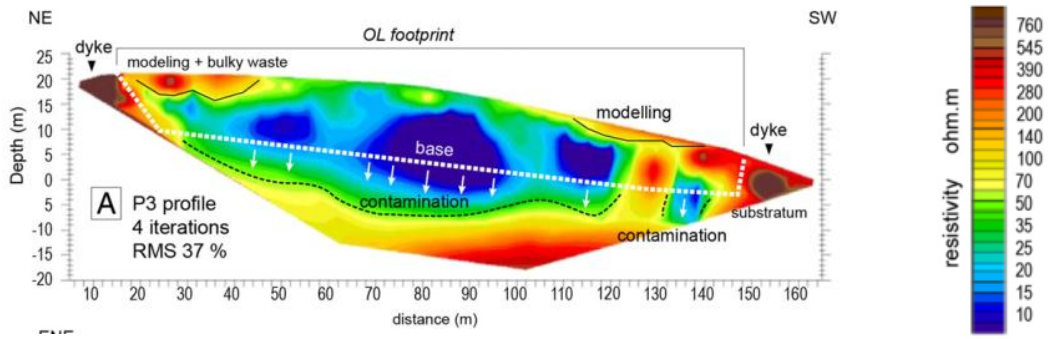

Figure 2.13 Landfill profiles to the southeast

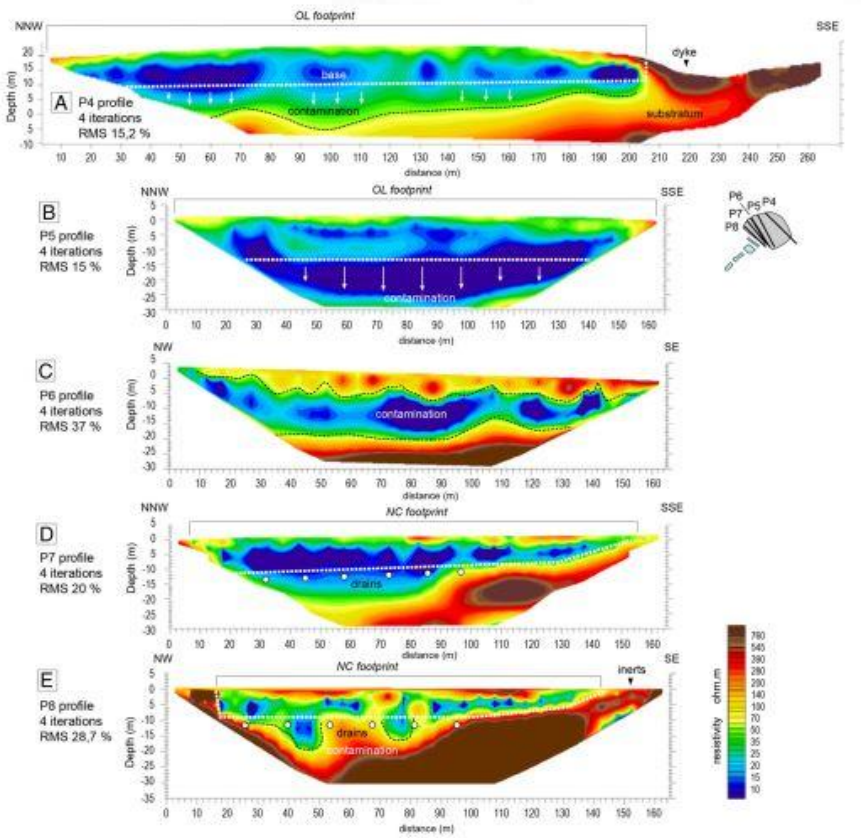

Figure 2.14 Landfill profiles over the old landfill: NW-SE (P3, P4, P5), Landfill profiles between the old landfill and the new cell(P6), Landfill profiles at the new cell (P7 and P8)

Research of Jolanta Pierwola, 2013 invested the soil contamination using resistivity and Induced Polarization at Poland. It is mine has a name is Bukow, located around 10l m south of Raciborz town, and around 170 m north of the Odra River. This waste dump is area, where took waste from the Rydułtowy-Anna coalmine since 1976. This area has an area approximately 45 ha and the waste material were piled up to 20 m high. The material of waste is about 90% coarse-grained. Lithologically including two main types are mudstones (70%) and dants. Because this is a stored waste, hence it is very low absorbability, high permeability. In detail, three geoelectrical surveys and one geological section were done around the lake. The first geoelectrical profile (with 200 m length of measurement) situated NE of waste, where is regarded uncontaminated water come. Other two profiles were located in the highest the ability of the polluted with 200 m, 100 m of length, respectively. Dipole - dipole was chosen to measure the value of resistivity and IP. The spaces between two electrodes of line 1, line 2 and line 3 were 5m, 5m, and 2.5m in turn. The current intensive was 10-200 mA, the decay time is 2s and the chargeability was checked in a ten-time window with 20 ms per time. Then, Res2Dinv software was used to obtain data. 50-150ms is the time was applied to analyze chargeability. The results showed that at sites has low resistivity (<15 Ohm-m) do not connect with increase chargeability, they are explained as areas of high infiltration of contamination. Combination with the geological section closes with the geoelectrical profile, the increasing values of chargeability is due to the appearance of Na^{+}, SO_4^{2-}, Cl^{-}, Mg^{2+}, Fe^{2+}, Fe^{3+}, and Mn^{2+} (Jolanta Pierwola 2013)

2.6 Heavy metal assessment using Geo-chemical

Geo-chemical analysis is a common method in evaluating the concentration and polluted level of sediment and soil. The Enrichment Factor (EF) in metals and Geo-accumulation Index (Igeo) are deliberated as indicators which applied to assess the existence and intensiveness of human contaminant deposition on subsoil. These indexes of capability contamination are computed by standardization of one metal concentration in surface soil compared with the concentration of reference component. A reference element is and a particular s element in the soil, which is

difficult to join to the atmospherical aerosols from human sources. It is better to the component chosen is connected with tiny particles (connect with grain size), and its concentration rarely affected by human effect.

The Enrichment Factor is demonstrated as bellow formula:

$$EF = \frac{(C_n/C_{ref})_{soil}}{(C_n/C_{ref})_{background}} \quad (12)$$

While:

C_n: Concentration of an examine element;

C_{ref}: Concentration of the reference element

Soil quality was assessed by EF index with different levels (Table 2.2) from Efficiency to minimal enrichment (EF<2) to extremely strong enrichment (EF>40).

In the first beginning, the Geoaccumulation Index (Igeo) was found out by Müller for concentration of metal in the 2-micron element and then was continuously grown to become a world standard value as below formula:

$$I_{geo} = \frac{lnC_n}{1.5 \times B_n} \quad (13)$$

While:

Cn: An examine element in soil dust;

Bn: The geochemical background concentration of the reference element

1.5 is the constant value (which demonstrated the natural variation in the content in the environment and to recognize the small anthropogenic influence. Müller has defined this formula with seven levels of Geoaccumulation Index (2.3) ranging from Level 0 (Igeo=0, unpolluted) to Level 6 (Igeo>5, extremely polluted) in 1981.

These are summaries classifications of Igeo and EF indexes:

Tale 2.3 Enrichment factor (Remeikaite-Nikiene et al. 2018)

Class	Value	Soil dust quality
1	EF<1	No enrichment
2	1≤EF<3	Minor enrichment
3	3≤EF<5	Moderate enrichment
4	5≤EF<10	Moderate severe enrichment
5	10≤EF<25	Strong enrichment
6	25≤EF<50	Very strong enrichment
7	EF≥50	Extremely strong enrichment

Table 2.4 Geoaccumulation index (Younis and Tesfamariam 2017)

Class	Value	Soil dust quality
1	Igeo < 0	Unpolluted
2	0≤Igeo<1	From unpolluted to moderately polluted
3	1≤Igeo<2	Moderately polluted
4	2≤Igeo<3	From moderately polluted to heavily polluted
5	3≤Igeo<4	Heavily polluted
6	4≤Igeo<5	From heavily polluted to extremely polluted
7	Igeo ≥ 5	Extremely polluted

To control the contaminated state of heavy metal and metalloid in exterior sediment of heavy metal in mining area for bauxite ore in Malaysia, the researcher gathered samples and computed a few indexes (The sediment enrichment factor (EF); The geo-accumulation index (Igeo); contamination factor (CF). Samples were collected by stainless steel trowel at seven sampling points in surface sediment, whereby (0-20 cm) surface into a plastic bag and then locked carefully by zipping.

While 4 samples were taken at the mine tailing and others were got nearly stream and an old mining pond stopped exploiting. They were protected in a cool box with ices (at temperature is under 4 ^{o}C) and transferred to the laboratory to analysis following EPA method 3050B (USEPA 1996). The outcome of Igeo index indicates that Fe, Al, Mn, Zn, Cr, Al, Co, Cd, and Sr are un-contaminated metals, however, Pb is shown moderate contamination at some places with Igeo results placed from 1, 2 thresholds.

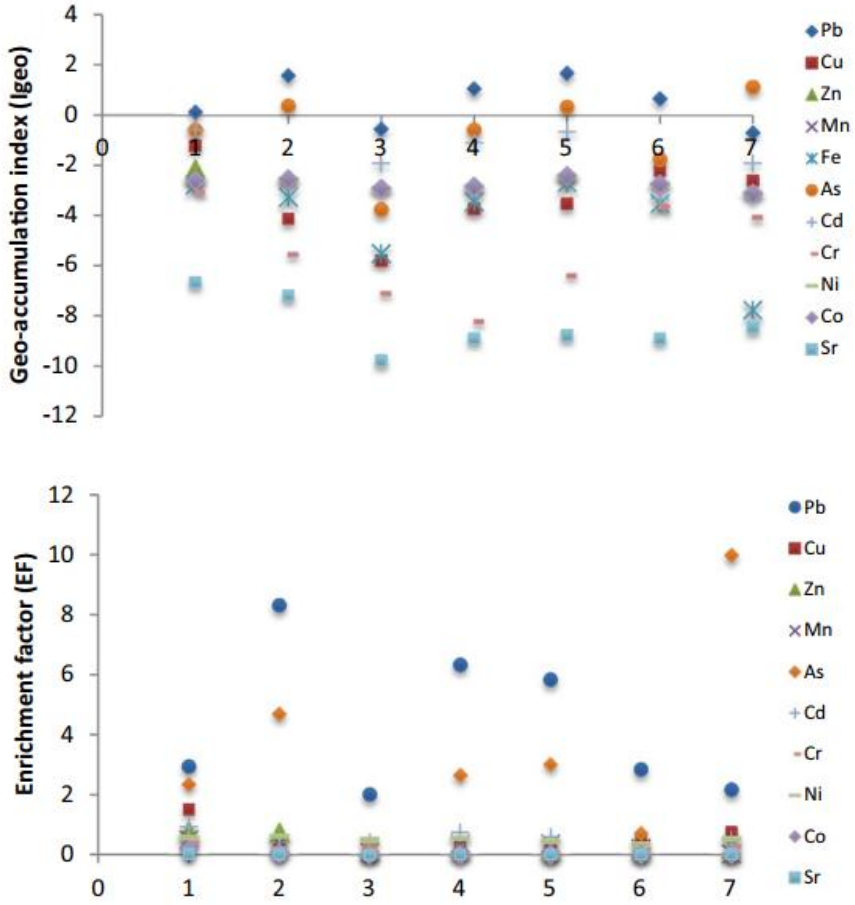

Figure 2.15 The result was similarly depicted with Igeo, Pb is proving are moderated contamination with index is from around 2 to 10 (Kusin et al. 2018)

In 2008, Lépold and his partners were successful (Léopold et al. 2009) when applying Geoaccumulation Index and Enrichment factor to evaluate the metal contamination in freshly deposited sediments between river Migoa and the Municipal lake of Yaaounde, Cameroon. From the lake to river Mfoundi connected to the Atlantic Ocean via River Nyong (including the main branch of the lake, the lake, and water) has three sections in the research area; 35 points were collected samples of

freshly deposited sediments (5-10 m) in the dry season (January, 2005). And then they were analyzed in the laboratory using ICP-AES (Perkins-Elmer Optima 3000XL) follow the settings of RF power 1,300 W, plasma flows 15 L/min, nebulizer flow 0.8 L/min in a laboratory of Korea University. The highest enrichment factor value with Pb is 125.77, Zn is 24.0), Cu is 21.98 and Co is 9.06 was found in Mingoa stream. Moreover, these results find the source of contamination base on the different EF values at other places. However, the main contaminated source is mentioned that it comes from anthropogenic inputs because the study area is the urbanized region and having a destruction of battery near to the lake lead to along to the whole water body they can find high EF value, especially with Pb, Cd concentration in lake are 125.77, and 311.78 respectively. Combine with Igeo index, which indicated that Igeo of Mn, Cu, Pb, Zn at some sites picked to a strong heavy metal polluted with Igeo of Mn, Cu (0-2); Igeo of Pb (0-3) and Igeo of Cd (2.89-5.12) (Léopold et al. 2009).

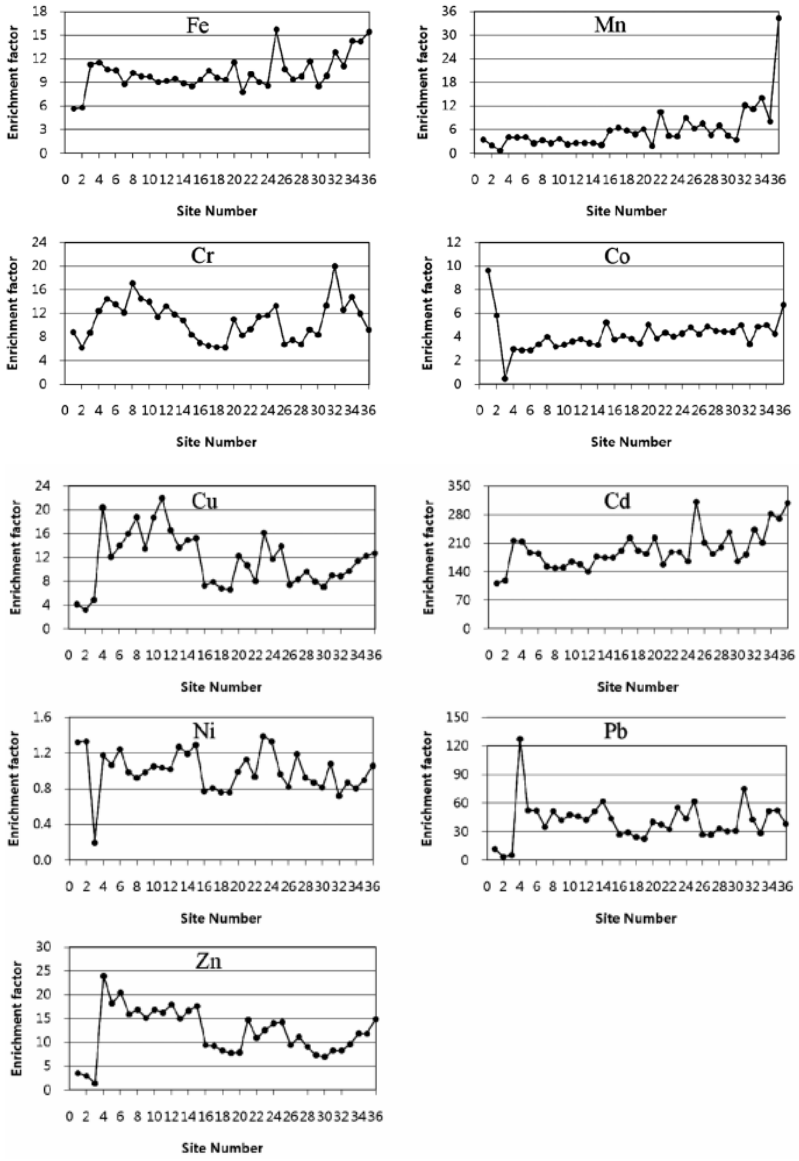

Figure 2.16 Variations of enrichment factors with sampling sites

2.7 Correlation Coefficient ("R") and Linear equation

a) Correlation coefficient

Correlation coefficient is calculated by a bivariate analysis, which describes the strength of opponent of two objects and the direction of the relationship. The range of coefficient varies from -1 to 1. The value indicates are ±1, seemed to be an accurate association between two variables. If the value of correlation coefficient value equal 0, the connection between two variables is very weak. Otherwise, the

direction of the relationship is shown through the sign of the coefficient with ± (Statistics How To 2019). A minus sign shows that a negative relationship and a plus sign illustrate a positive relationship (Lærd statistic 2019). Normally, in statistics, the most popular types of correlations are Pearson correlation, Kendall rank correlation, Spearman correlation. A linear relationship of two variables is a particular situation of a monotonic relationship (Statistics How To 2019). Normally, this coefficient is applied in the context of a linear relationship between two random variables or two continuous variables and it is regarded as a Pearson product-moment correlation. The correlation coefficient is interpreted with a few ranks as "weak", "moderate" or "strong" relationship (Schober et al. 2018), a conventional approach to clarify the correlation coefficient is given in the table below :

Table 2.5 Conventional Approach to Interpreting a Correlation Coefficient (Schober et al. 2018)

Correlation Coefficient	Interpretation value
0-0.1	Slight correlation
0.1-0.39	Weak correlation
0.4-0.69	Moderate correlation
0.7-0.89	Strong correlation
0.9-1	Very strong correlation

Pearson correlation: This is the most popularly used correlation statistic to assess the level of the relationship between linearly connected variables. Both variables is distributed around a straight line (Statistics How To 2019).

$$r = \frac{n(\sum xy) - (\sum x)(\sum y)}{\sqrt{\left[n\sum x^2 - (\sum x)^2\right].\left[n\sum y^2 - (\sum y)^2\right]}} \qquad (14)$$

Where:

r : Pearson correlation coefficient

N : number of cases

$\sum xy$: the sum of the paired values (x, y)

$\sum x$: the sum of x values

$\sum y$: the sum of y values

$\sum x^2$: the sum of squared x values

$\sum y^2$: the sum of squared y values

Kendall rank correlation is a non- parametric examination that estimates degree of Kendal rank correlation of two variables (Statistics How To, 2019). For instance, we have two samples a and b, where every sample size is n, amount of pairing with a and b is n(n-1)/2. Base on formula, Kendal rank correlation is computed:

$$\tau = \frac{n_c - n_d}{\frac{1}{2}n(n-1)} \quad (15)$$

n_c: number of concordant

n_d: Number of discordant

Spearman rank correlation is a non-parametric test and it is useful to appraise the relationship of association between two variables. This formula is calculated on a scale that is at least ordinal but doesn't use any distribution of the data (CompleteDissertation 2019).

The Spearman rank correlation is used to calculate as below computation:

$$\rho = \frac{6\sum d_i^2}{n(n^2-1)} \quad (16)$$

ρ : Spearman rank correlation

d_i: : The difference between paired ranks

n : Number of case

b) Linear equation

A linear equation shows a correlation in two variables which the value of one of the variable depends on the value of the other variable. Example x, y are the two variables while x is the independent variable, y is the dependent variable. A linear equation can find out the y base on a value of x as a pair (x,y). A linear has form $y = mx + b$ (MathStep 2018).

A linear relationship (or linear equation) is used to forecast the unknown value of variable X using the defined value of variable Y.

CHAPTER 3
METHODOLOGY

3.1 Study area description

Saphan Hin coastal placed in Wichit, Mueang Phuket District, Phuket, Thailand. This is the open area for everyone from young children to old people. This destination is considered as seaside park of Phuket town with many attractive places such as Saphan Hin beach, Saphan Hin stadium. Around 4 pm onward, at the stadium, many sports activities are organized by individuality or group as playing badminton, basketball, tennis, football or swimming. Furthermore, Saphan Hin is the perfect place for picnicking, doing exercises or relaxing. The weather at Phuket is very wonderful with typical tropical weather; the average temperature is annually from 30-33 ^{0}C. The rainy season caused by the Monsoon extends from June to December, and the dry season is from January to May with a medium annual rainfall of 2,314 mm ("Climate", n.d.). Thai and Chinese are the most popular here, besides this is attracted tourism with the amount of foreigner tourist from many countries in the world. However, the research area (Figure 1) is a coastal zone placed next to the built land, named Saphan-Hin situated in the southeastern region of Phuket Island, with coordinates 07º51'38.6" N and 98º24'07.9" E (Weesakul and Lowanichchai 2005). Moreover, Mueang is the district has long historicity with exploiting tin mining. Hence there are many opinions consider that the research is related to the tin mining waste.

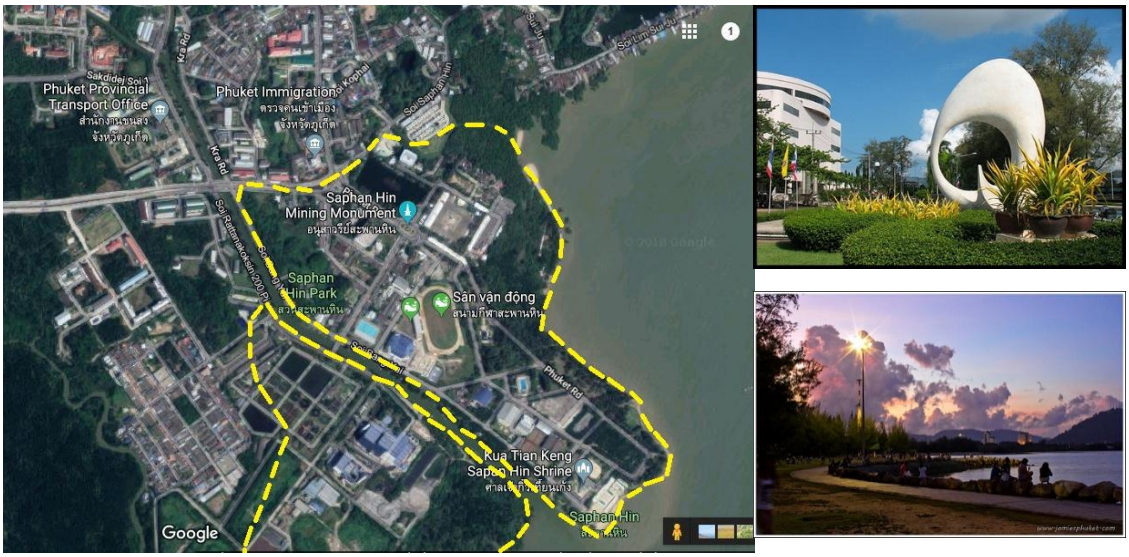

Figure 3.1 Saphan Hin coastal view: an odd-shaped monument in the center of a traffic circle; a nice park with paths for walking (the place is encompassed by yellow line seems to be the constructed area)

3.1.1 Geological and Hydrological Setting at Saphan Hin

3.1.1.1 Geological sitting

In Phuket, metamorphic rock, igneous rock, and sedimentary rock occupy as the bedrock and alluvial deposits (Brown et al. 1951). The geological condition of Phuket Province divides into two, the lower formation and upper formation and eight major rock groups. They are Carboniferous-Permian granite, Jurassic-cretaceous granite, Jurassic granite, volcanic rock and other intrusive rock, sedimentary rock (clay, calcium, and lime), metamorphic rock, quaternary sediment, and limestone (Soralump 2010). The metasedimentary rocks outcropped in the North on the east side, black slate or shale containing scattered pebbles is exposed. The pebbles are of quartzite, siliceous slate, and medium-grained biotite granite. Geology system at the research area is very varied with many types of soils such as CPk, Kqr, Qa, Qc, Qmc, Qms. However, based on the borehole results, structure geology of Saphan Hin is illustrated with main ingredients as soil, clay at the top from 0-15 m; deeper than 15 m are stone or stone decay, and finally granite, black rock or bedrock located at 30-60 m depth.

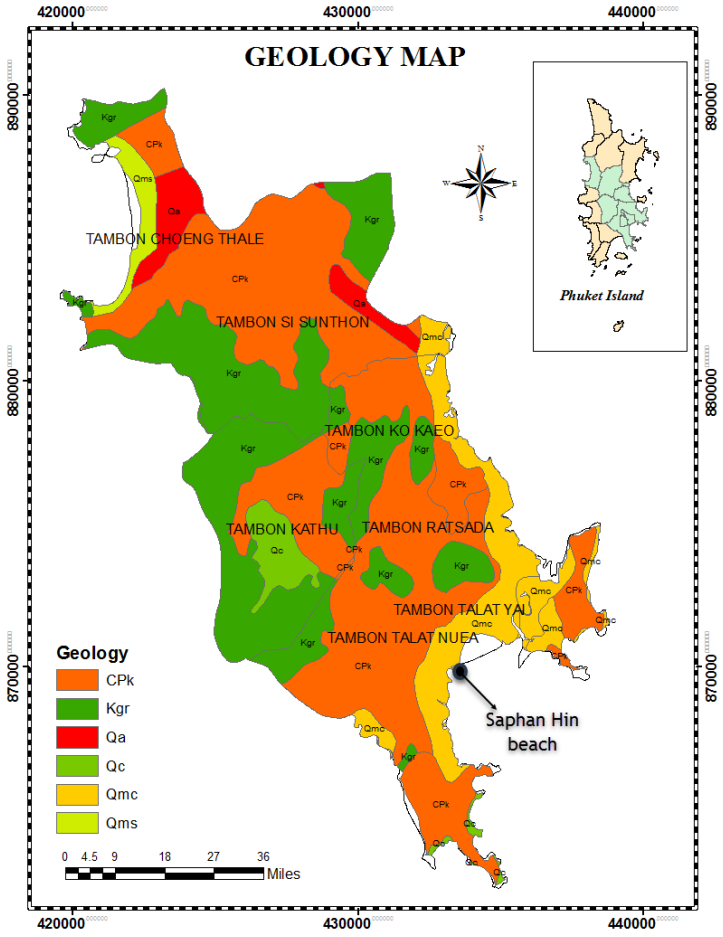

Figure 3.2 Geology map

3.1.1.2 Groundwater level

By the time, natural and anthropogenic factors have been reducing the groundwater level in Phuket as over-pumping of groundwater, reduction annual precipitation caused by climate change, urbanization. Base on the collected data from the government website, the average groundwater at Phuket is 11meter under subsurface (Sakanann 2017). In the study area, the groundwater level is about from 5 to 10 m.

Table 3.1 Groundwater data of Muaeng district, Phuket Island

Name	X(Easting)	Y(Northing)	Groundwater level (m)
546G024	430504	868928	4
5.506E+43	430384	868809	2
TQ99	430469	868837	8.5
TQ148	430482	868929	10.2
TQ40	430277	871322	3.2
TQ305	430301	871268	6
5406G004	430081	871901	3
TQ297	430705	872004	6.5
TQ190	432560	866715	18
5506F049	432701	866852	10
DCD16062	434814	862385	5
TQ270	433654	863931	18

From the data, an estimation groundwater level for Saphan Hin area is created as below map:

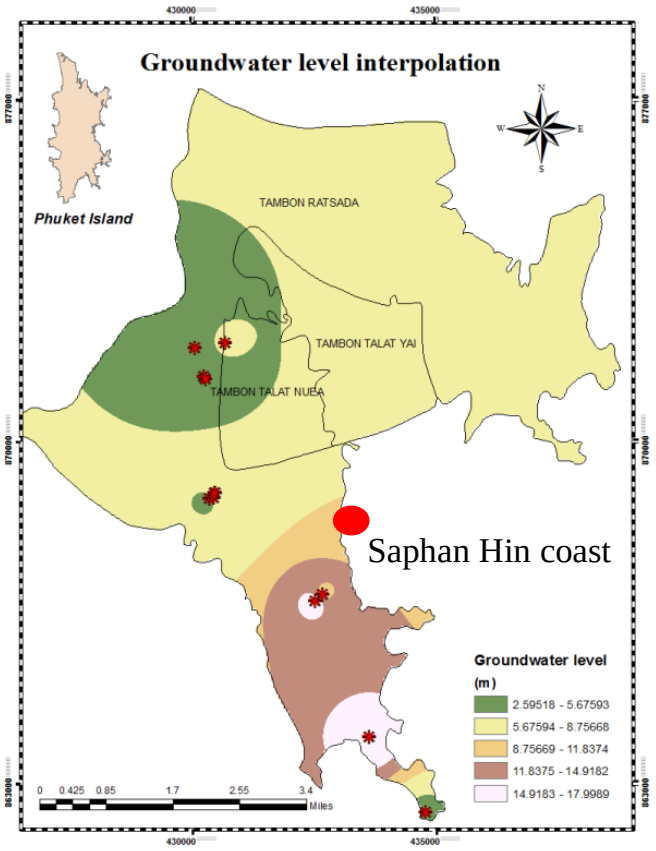

Figure 3.3 Interpolation groundwater level map

3.1.2 Population

As the collected data in August 2016, there is about 392,011 people live in Phuket Island. Population density here is nearly 722 people per kilometer square. But people mainly live in coastal zones and south of Phuket. Because this island is a tourism paradise thus parts of people are very varied with the amount of foreigner not only Asian as China, Korea, Japan but also Europe, an American tourist. According to data of the National Statistical Office (2017), the survey of Immigration Department predicted that by 2019, Phuket will continuously welcome approximately 14,382 working foreigners and about 78,734 migrant people. According to the Mueang is the district has highest population number with population density is 1044.4 people per kilometer square, 1.3 times higher than Kathu district (with 831.9 people per kilometer square) and nearly 2.7 times higher than Thalang district (with 395 people per kilometer square). At Saphan Hin, a huge amount of people are

Chinese. They live and establish the streets where is a rich custom and culture characteristic of China.

3.1.3 Activities are seemed to be factors affect heavy metal contamination in the study area

3.1.3.1 Abandon tin mining

In 1528 A.D, the era of Siamese King Ega Thodsarot, tin mining industry developed in Phuket and it became a major export and Portuguese taken place as a sole agent for the tin trade. Managing these tin mines was done by French company. In 1809, the tin mineral was found at Kathu and then Chinese migrated to Phuket and started numbers of tin mine operating (Siripong 2013). During those prosperous years, Phuket town really developed due to miners and for this century, tin mining has been very important to Phuket but in the year 1980s, tin mining was stopped entirely because of the Phuket local people joined other works to make money, including farming, fishing and now tourism. So, this past activity left about 300 abandoned mining reservoirs around Phuket Island. Tin mining causes a high disturbance in the environment as well as affects the local people who live in the countryside of Phuket (Easy Day Phuket 2013).

Bang-Yai is a small canal, belongs Saphan Hin sub-district. This is primary water with using purpose is main transport goods into Phuket town before. The water resource is provided for Bang-Yai canal is principally from a reservoir upstream at Kathu waterfall through abandon Tin mining area and Phuket town into the coastal zone at Saphan Hin. Therefore, the water source is transferred through Bang Yai is assessed to be a main contaminated source.

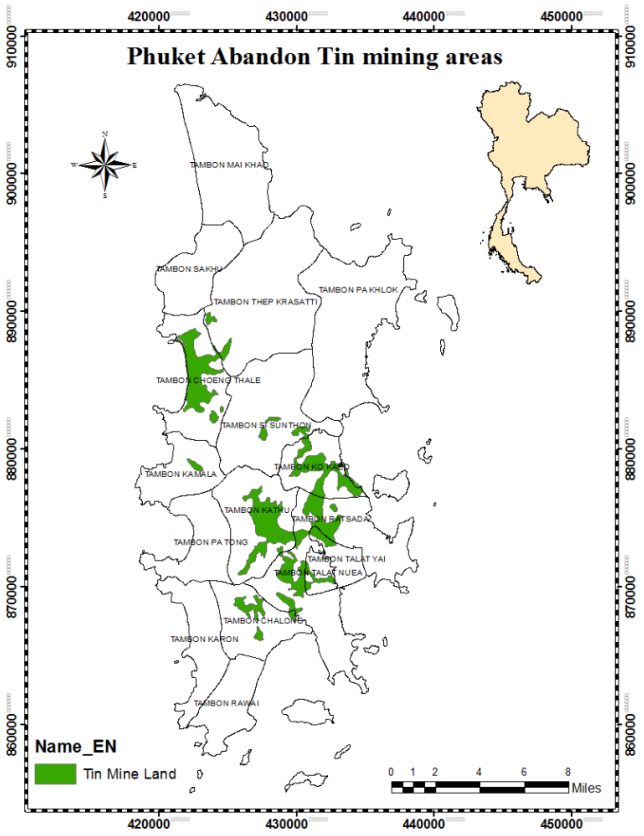

Figure 3.4 Abandon tin mine places map

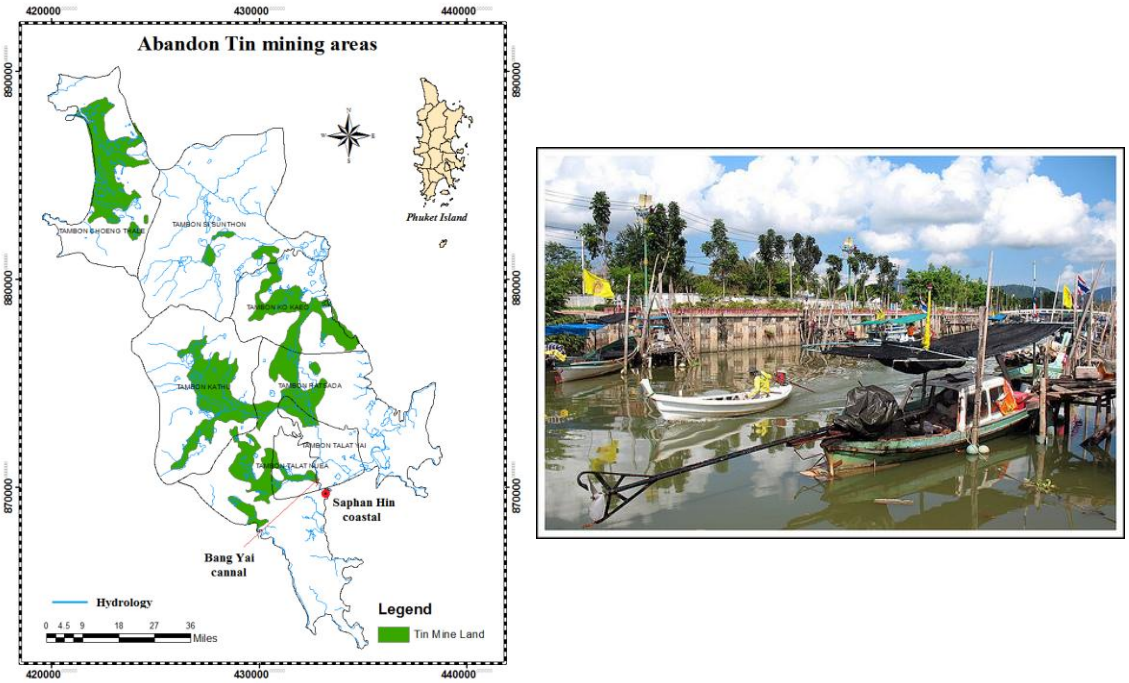

Figure 3.5 Hydrology system in the research area (left); Bang Yai canal (right)

3.1.3.2 Incinerator

Near to the Saphan Hin coast, the end of Bang Yai canal, at coordinate 433140E; 869100N a large incinerator has built and started to work since 2012 to tackle with increasing waste and trash by locals and the tourist service with a total area is over 465.600 m^2 and construction cost is 994 million Baht. Averagely, this factory handles about 700 tons of waste per day. The temperature of the incinerator is kept at 850-900^oC, continuous combustion is 7,000 hour per year and maximum production is 2.5MW. Waste, trash in all Phuket is collected and transport to here to treat including domestic trash, waste of factories. This processing system is divided into three main sections: Section A is landfill area (5 zones), with about 21,400 m^2, containing all collected waste. Sections C is an incinerator burning and treating waste after being gathered, section B is a place to keep wastewater treatment area and finally, area is buffer to protect for factory with area 20 m^2. Although incinerator is quite a modern method in treating waste it is not the radical method with some issue output as air pollution, landfill of ash or landfill leachate.

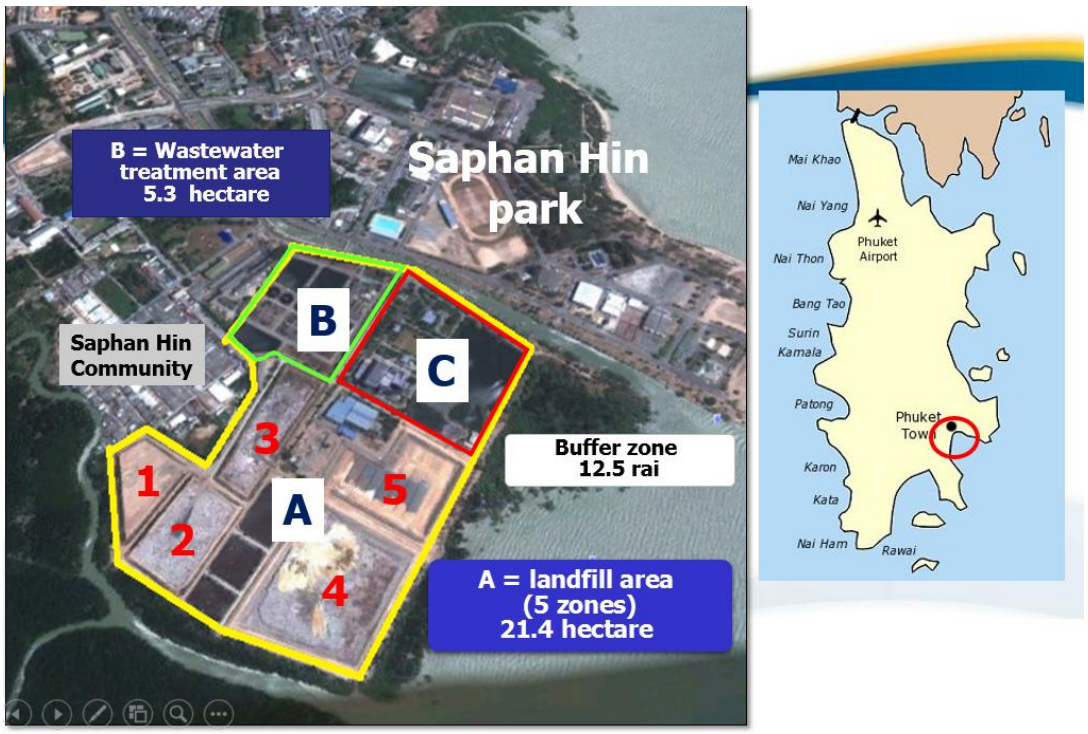

Figure 3.6 Incinerator Place

3.2 Materials and Methodology

The main purpose of this research is finding the source of heavy metal and investigating the level of pollution, therefore Geo-electrical resistivity imaging and geo-chemical analysis will be done together even though every method has own function. This picture below show briefly overview methods of their objectives.

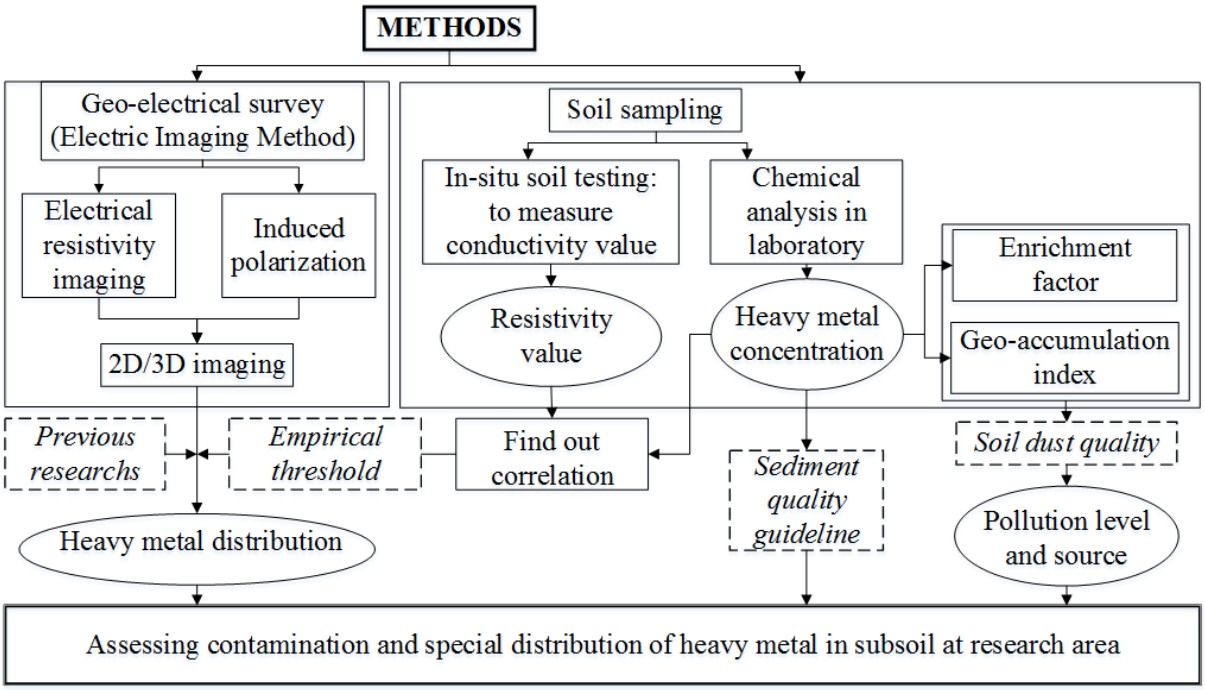

Figure 3.7 Summary methodology

Geo-electrical surveys are implemented for four lines, sited at around coastal Saphan Hin and a part of Bang Yai canal including four lines: Line 1a, Line 1b, Line 2a, Line 2b. This was employed to demonstrate the subsoil considerable pollution from the heavy metals source connected with abandoned mining activities in the surrounding area of Bang Yai estuary upstream to coastal territory. Similarly, Geo-chemical was done to analyze and assess the level contamination of research area.

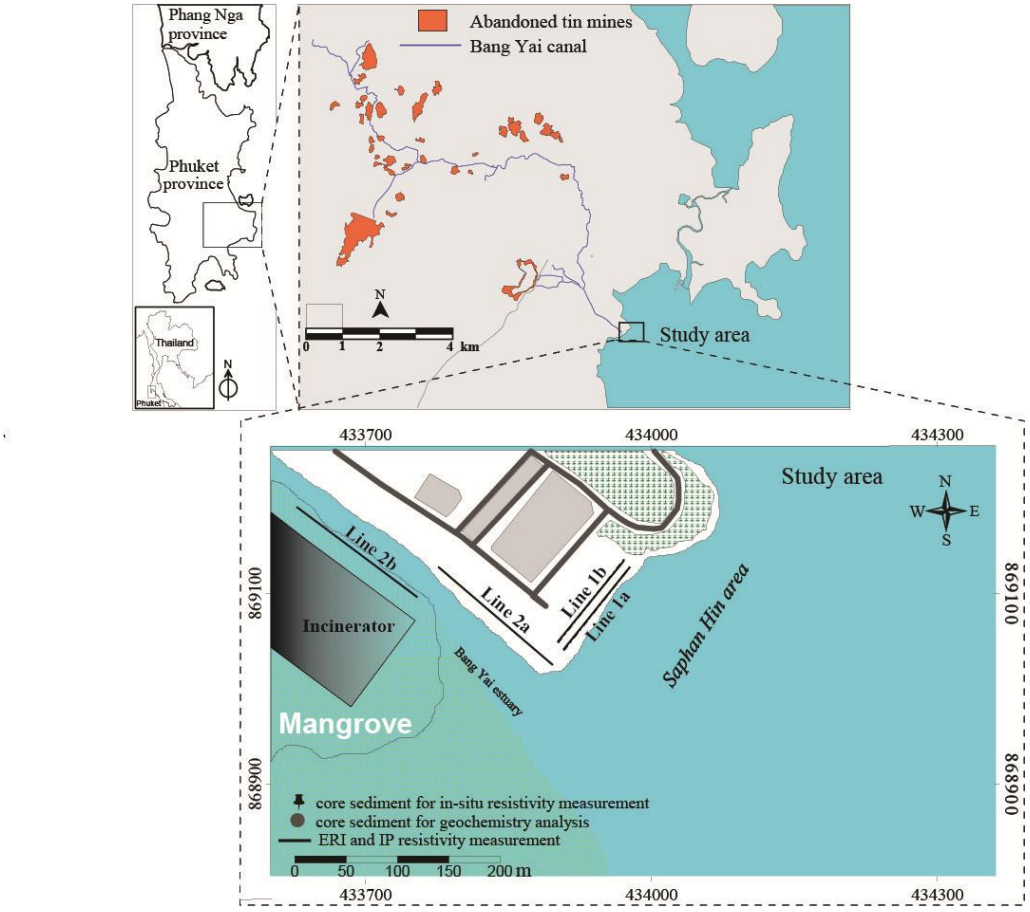

Figure 3.8 ERI measurement and core sediments places

3.2.1 Electrical resistivity imaging (ERI)

Geo-electrical surveys, i.e., ERI and IP methods, were implemented by using AGI SuperSting R2. This equipment connected with multi-electrodes system (56 electrode channels) and used to measure both resistivity (R) and induced polarization (IP) of materials of subsoil.

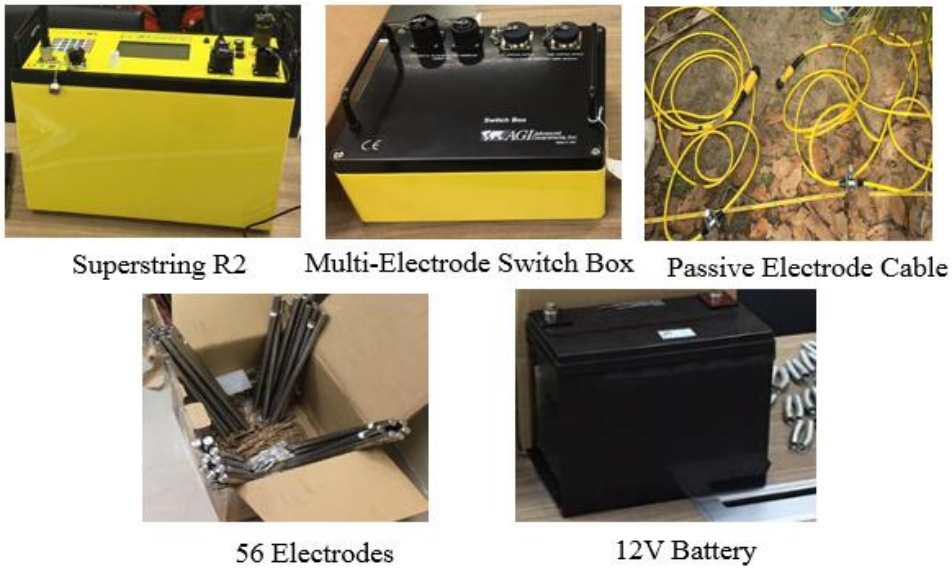

Figure 3.9 List of equipment for ERI survey

Four line surveys were conducted to find the change and trend of resistivity value from the area, where have abandoned tin mining to estuarial, incinerator and coastal area through two main stations, such as:

+ Along Bang Yai canal region (around 2.5 km), two lines (line 2a, line 2b) are designed and arranged parallel to canal and close to the incinerator.

+ Around Saphan Hin coastal region including two parallel lines (line 1a, line 1b). Two lines are parallel to coastal line combined and established 3D imaging to observe the simulation of contamination from coastal zone to inland. Otherwise, originally Saphan Hin is not natural construction but it was built by human's design in the past. Or the heavy metal contamination could come from this building activity. The site of every line was defined and recorded by GPS with the first and the last electrode. The received information from GPS was verified and compared with processing and inversion process by using 2D/3D Earth Imaging. Wenner configuration was applied for all lines in this research because Wenner configuration is effective to vertical changes and can limit the maximum noise of resistivity value (Uchegbulam and Ayolabi 2014).

Table 3.2 Geo-electrical survey lines

No.	Name lines	X	Y	Elevation (m) (MASL)	Space between two electrode (m)	Collected depth (m)	Note
1	Line 1a	433933	869094	6	2	~ 20	Close with the sea
2	Line 1b	433933	869094	6	2	~ 20	Close with the sea
3	Line 2a	433680	869206	8	5	~49	Perpendicular with coast
4	Line 2b	433261	869426	7	5	~49	Near to incinerator

Running ERI survey and collecting samples at research area were separated to many times because average a day, to get resistivity and IP value, for instance, one line (with space interval between two electrodes is two meters or five meters) need from around three to four hours hence with seven profiles the work will be done from four to five days.

All ERI profiles were conducted with a different length to suit to the terrain of every research place (The mean sea level of lines is collected by GPS to get high accurate). EarthImager 2-dimension and 3-dimension were used to do resistivity and IP data inversion by using finite-difference method. The resistivity and IP inversion were inverted separately. The inversion process attempted to integrate the measured and calculated model. The 3D-ERI was done through combining two 2D-ERI lines (Line 1a and Line 1b) with the distance approximately 40 m. In terms of 3D inversion, the visualization of cube was presented to be confirmation information in order to depict the conductive plume over time.

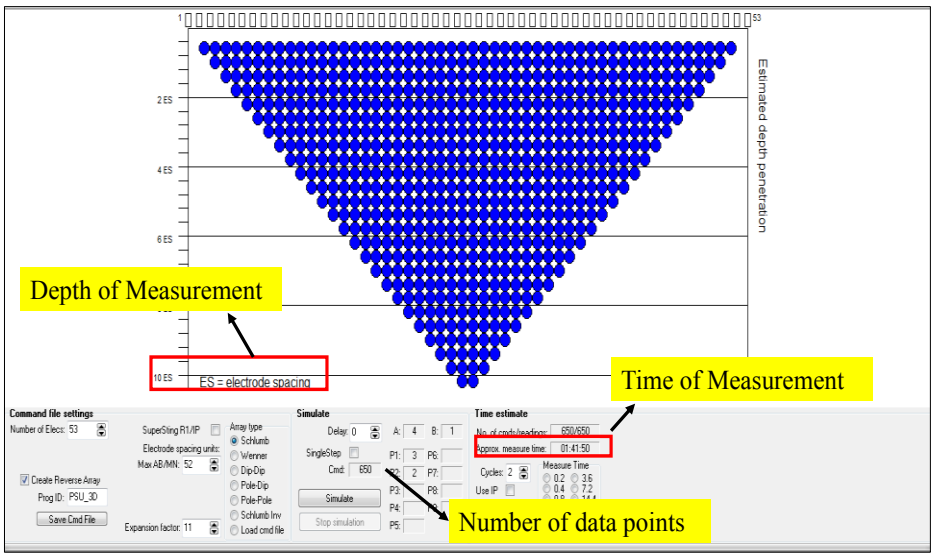

Figure 3.10 Surveyed line of ERI designed by using simulation

3.2.2 Soil sample analyzing

The number of soil samples will be taken at the sediment area in Saphan Hin coastal with twelve cores. Among them, five core (core I, core II, core III, core IV, core V) are analysis heavy metal in the laboratory and seven cores (S1, S2, S3, S4, S5, S6, S7) were taken around core I, core II, core III to measure resistivity value. Hand auger (Russian-corer) is the tool used to take the sediment sample at the beach. Each borehole will be dug to 51 cm from surface and then classified at every ~3 cm depth interval. Taking sample was prepared carefully and done in a good weather condition: not raining, sunny or cloudy and wait until low tide. The divided samples were kept in black plastic bags and preserved in a box with cold temperature to diminish potential contamination and transported to the laboratory.

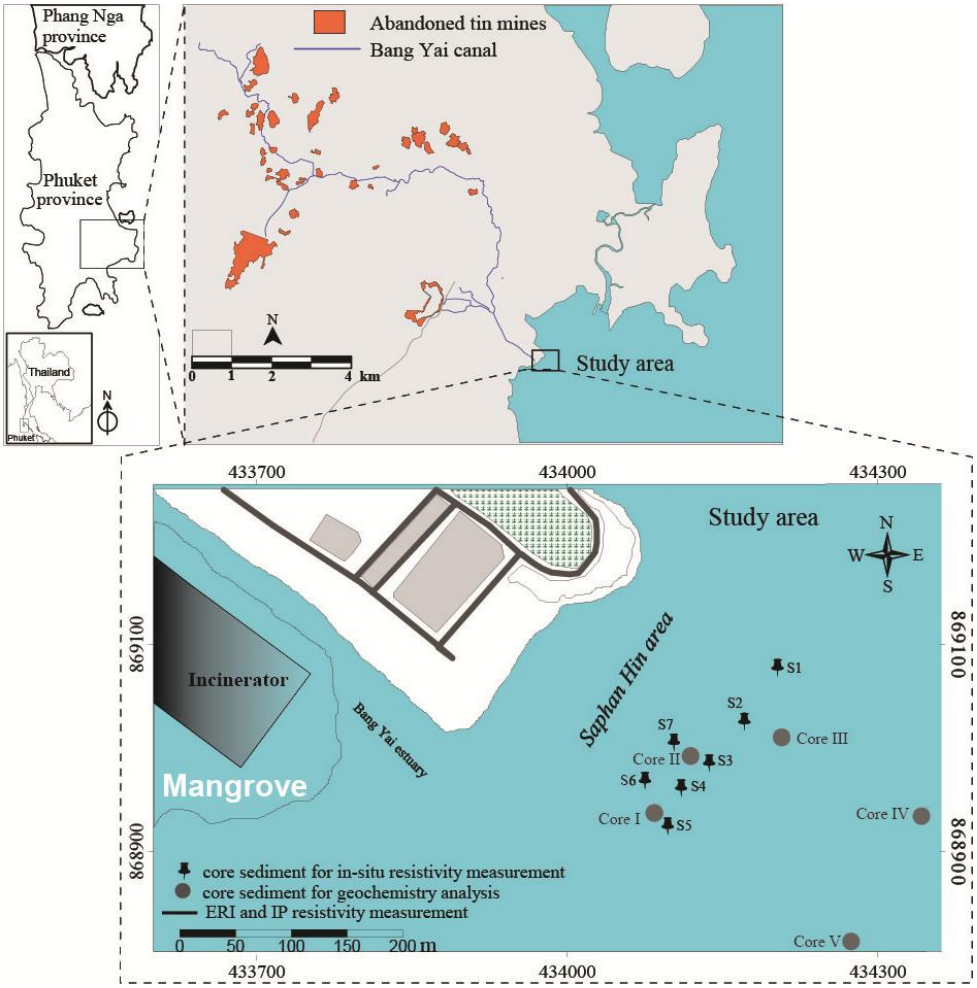

Figure 3.11 Geo-chemical soil sample sites

The collected sample was separated into two groups

Group 1: Doing in-situ measuring conductivity value with seven cores (S1, S2, S3, S4, S5, S6, S7).

Group 2: Measuring the concentration of heavy metal contamination in the laboratory.

a) In-situ conductivity testing

Conductivity will be checked by using a HANNA HI-9813-6. Before testing conductivities value, equipment will be cleaned with distilled water and adjusted with standard calibration HANA instrument – conductivity solution HI70031 (1413 $\mu S/cm$). Doing similarly with next samples and write the results cautiously.

Figure 3.12 HANA HI-9813-6 equipment

b) Heavy metal concentration analysis

The other samples are determined the major cations of coexisting heavy metals (Zn, Pb, and Cu) and the analytical technique using for the determination is aqua-regia (Potts 1987). Every core was separated into smaller part with 3cm per core. Then, the sample they dried at 60-80ºC and sieved with different diameter: <63 µ, 63 µ - 150 µ, ≥ 150 µ. With smaller 63µ diameter sample, 0.02g sample weight was taken and digested by the EPA method 3052 (EPA 1996).

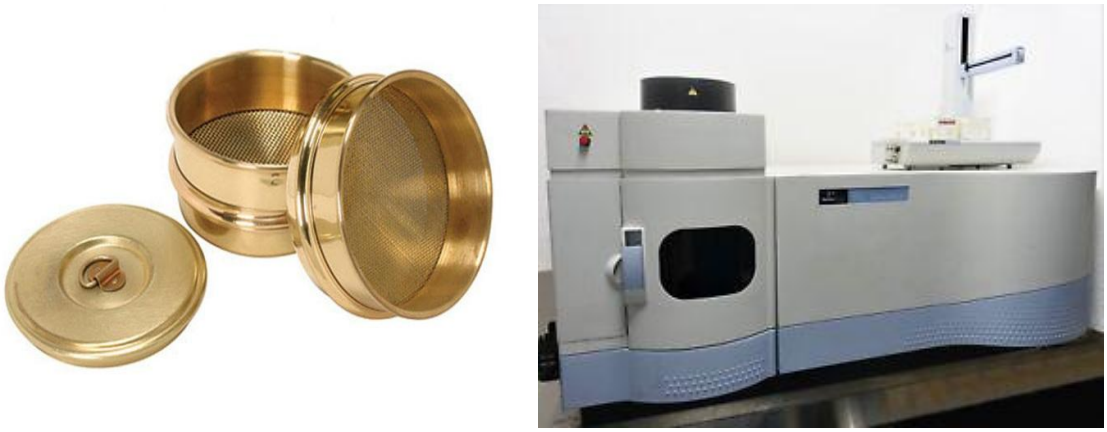

Figure 3.13 Soils analysis equipments (sieves, Perkin Elmer Optima, 4300 DV/Perkin Elmer Optima 800)

Next step, analyzing the concentration of Zn, Pb and Cu were checked by Inductively Coupled Plasma Optical Emission Spectrometry (ICP-OES) (Perkin Elmer Optima, 4300 DV/Perkin Elmer Optima 800). This method is proved that it is accurate and sui with trace metals and other constituents (MESS-4) by applying the marine sediment reference material (NRC 2014). Subsequently, analyzed Pb, Zn, and Cu concentration in the laboratory were compared heavy metal concentration standard in the world. Depend on the countries the safe threshold of concentration of Pb, Zn and Cu are different. Some countries classified the standard of heavy metal concentration as table below:

Table 3.3 Reference heavy metal concentration value of Pb, Zn, and Cu in some countries

Pollutants	**contents of average heavy metals in few moderately contaminated coastal zones (mg/kg)**						
	A*	**B***	**C***	**D***	**E***	**F***	**G****
Pb	138	20-296	32-88	20-120	33-80	21-83	50
Zn	234	61-338	100-274	80-180	34-67	56-210	200
Cu	61	21-343	53-105	7-18	15-31	21-71	65

** A: Cardiff Bay (England), B: Medway Estuary (England), C: Pearl River Estuary (China), D: Surface sediment of the Mejerda Delta, E: Persian Gulf, and F: Gdansk Basin (Poland) (Helali et al. 2016); ** G: Australia (Wafi 2015)*

Or other examples is Sediment quality guidelines (SQGs) - standard guideline appropriate to assess the polluted level of heavy metals in marine sediment (Sharifuzzaman et al. 2016)

Table 3.4 Sediment quality guidelines (SQGs) - standard guideline applicable for heavy metals (Pb, Zn, and Cu) in marine sediment

Sediment quality (mg/kg)	**Pb**	**Zn**	**Cu**
Average quality in crust	12.5	70	*55*
Non-contaminated	<40	<90	*<25*
Moderately contaminated	40-60	90-200	*25-50*
Heavily contaminated	>60	>200	*>50*

Igeo and EF are two indicators, applied to simplify the cases of heavy metal contamination in the coastal sediment through below formulation:

$$\text{Igeo}=log_2\left(\frac{C_n}{1.5\ x\ B_n}\right) \text{ (Müller 1981)} \quad (17)$$

Where:

Cn: A concentration of examine element in soil dust;

Bn: The geochemical background concentration of reference element

$$\text{EF}=\frac{(Cs/Cnorm)_{sample}}{(Cs/Cnorm)_{background}} \text{ (Remeikaite-Nikiene et al. 2018)} \quad (18)$$

Where:

Cs: Concentration of an examine element (the sediment);

Cnorm: Concentration of the reference element

Commonly, normalizer used to compute EF index is Fe, Al (González et al. 2018) or, Mn, and Rb (Barbieri 2016)

At Phuket, the concentration of Pb, Zn, Cu in the shale were 20 mg/kg, 80 mg/kg, 10 mg/kg respectively. And Al is an element, practiced as a normalizer with 115360 mg/kg (Garson et al. 1975).

3.2.3 Validation of resistivity and Heavy metals concentration and find the empirical threshold for resistivity value

Finding the relationship between heavy metal and resistivity is the important one of the steps in this research. Conductivity values after being tested with HANA equipment will be converted to resistivity value follow this formula:

$$resistivity = \frac{1}{conductivity}$$ (Bayram and Maraşlı 2018) (19)

Where, conductivity (mho - Siemen) and resistivity (ohm)

At the same depth, resistivity value and heavy metal concentration were plot using the Pearson formula and set up the linear equation. Otherwise, the relationship between heavy metals (Pb, Cu, and Zn) was computed and plotted in graphs. Nevertheless, validation of resistivity and heavy metals concentration play an important part in setting a value for resistivity value to applying ERI method for all process. However, because of lack of Cu data in few cores, therefore only Pb and Zn were combined with resistivity value to find the correlation coefficient and linear equation between heavy metal concentration and resistivity. Although each country has a special standard to assess the heavy metal contamination for sediment, in this research, SQGs guideline was unified and used as a reference source in the assessment process at Saphan Hin coastal area. After establishing the linear equations of two variables (Pb, Zn concentration and resistivity value), the standard value of Pb (40 mg/kg) and Zn (90 mg/kg) in SQGs guidepost calculated back resistivity values. Finally, the average of all resistivity values was seemed as an empirical index to apply for set up scale in 2D Electrical resistivity image.

CHAPTER 4
RESULTS AND DISCUSSIONS

4.1 Geochemical results

4.1.1 Pb, Zn, Cu heavy metal concentration

Table 4.1 Heavy metal concentration and resistivity value

Core	Depth (cm)	Pb (mg/kg)	Zn (mg/kg)	Cu (mg/kg)	Al (mg/kg)	Resistivity (Ohm-m)
Core I	1.5	12.12	34.96	17.50	33735.52	2.26
	5.75	20.73	42.36	14.60	42718.69	3.50
	9	33.00	58.60	19.70	75745.15	1.85
	13.5	27.50	45.42	15.20	66188.37	1.55
	18	30.58	55.27	19.70	83012.67	1.49
	23.5	29.32	51.51	16.90	86188.51	1.36
	29	69.11	90.96	40.60	167025.81	1.32
	33	35.44	59.89	20.50	91050.61	1.65
	37	50.06	65.54	28.70	120907.04	1.53
	41	28.59	51.37	17.60	72888.05	1.52
	45	30.38	50.32	17.60	81523.47	1.81
	49	24.18	38.65	12.00	58346.56	1.49
Core II	3	12.38	45.43	-	21380.4724	2.54
	6	15.05	47.85	-	33566.6369	2.22
	9	20.24	57.75	-	47207.8952	1.85
	12	18.28	51.62	-	43193.3747	1.43

Core	Depth (cm)	Pb (mg/kg)	Zn (mg/kg)	Cu (mg/kg)	Al (mg/kg)	Resistivity (Ohm-m)
Core II	18	23.07	51.30	-	70778.9896	1.56
	24	26.26	62.09	-	65121.5585	1.34
	27	26.57	66.82	-	59579.6315	1.37
	30	29.62	64.39	-	76335.5149	1.79
	33	30.67	61.71	-	72105.3018	1.69
	36	29.93	63.40	-	93428.9763	1.51
	42	25.97	78.74	-	85219.1496	1.35
	45	19.25	62.44	-	55625.4939	1.61
	51	27.68	58.24	-	93759.2626	1.36
Core III	3	11.07	31.95	10.5	28818.4308	2.37
	6	18.23	49.62	16.2	56918.6754	2.43
	9	18.94	54.96	16.7	65721.6046	1.99
	15	31.50	63.04	25.1	93942.982	1.64
	18	30.94	55.34	22.3	107079.853	1.59
	24	47.48	68.92	26.7	133111.186	1.49
	27	63.02	71.85	25.8	169329.141	1.64
	33	54.30	66.28	28.4	152994.415	1.61
	42	45.32	67.90	27.9	140736.404	1.79
	45	39.06	61.76	22.4	139220.557	2.29
	51	40.32	61.88	25.5	139016.34	1.71
Core IV	1	7.99	24.00	7.61	23455.05	-
	5	7.46	27.37	5.78	24387.53	-

Core	Depth (cm)	Pb (mg/kg)	Zn (mg/kg)	Cu (mg/kg)	Al (mg/kg)	Resistivity (Ohm-m)
Core IV	10.5	12.25	44.77	9.99	40959.66	-
	16	10.59	33.75	9.15	38843.84	-
	20.75	18.52	59.47	15.98	76288.29	-
	26.5	29.97	78.02	15.44	91740.46	-
	31	53.86	69.14	24.57	147527.35	-
	35.5	51.55	68.00	24.79	146852.87	-
	40	57.85	70.34	27.59	152963.28	-
	45.25	33.00	55.01	18.24	97909.84	-
	50.5	31.91	52.42	16.50	100431.46	-
Core V	1	8.80	24.86	-	15041.65	-
	3	8.64	25.64	-	14821.51	-
	5	8.86	25.86	-	15612.95	-
	7.5	9.68	29.55	-	19734.19	-
	10.5	17.48	43.72	-	46748.91	-
	13.5	18.13	48.20	-	56334.44	-
	16	21.83	56.42	-	79290.59	-
	18	25.30	65.86	-	94553.08	-
	20	25.04	65.82	-	86787.10	-
	22	24.99	57.35	-	84102.95	-
	24	24.89	50.32	-	88515.01	-
	26	27.12	53.24	-	101200.52	-
	28	28.02	58.50	-	101955.52	-

Core	Depth (cm)	Pb (mg/kg)	Zn (mg/kg)	Cu (mg/kg)	Al (mg/kg)	Resistivity (Ohm-m)
Core V	30.5	25.85	50.45	-	95061.86	-
	33.5	34.35	70.03	-	122593.32	-
	36.5	28.42	59.86	-	91400.47	-
	39.5	40.15	74.36	-	136629.83	-
	42	49.86	84.60	-	193576.66	-
	44	38.32	79.77	-	128079.58	-
	46	27.93	62.01	-	87768.33	-
	48	27.96	55.33	-	85494.97	-
	50.5	28.74	64.69	-	114354.95	-

Concentration of Pb in sediment changed from 12.2 to 69.1 mg/kg, 12.3 to 30.7 mg/kg, 11.1 to 63.0 mg/kg, 7.5 to 70.3 mg/kg and 8.6 to 49.9 mg/kg, for core I to core V, while concentration of Zn in sediment altered from 35 to 90.96 mg/kg, 45.4 to 66.82 mg/kg, 31.95 to 71.85 mg/kg, 24 to 78.02 mg/kg and 24 to 79.8 mg/kg, for core I to core V. Concentration of Cu varied from 12 to 40.6 mg/kg in core I; from 10.5 to 28.4 mg/kg in core III and between 7.6 and 27.6 mg/kg in core IV. The maximum values of detected Pb, Zn, and Cu in very core often gather in the depths from 27 cm to 33 cm in table 4.2.

Table 4.2 Highest concentration of Pb, Zn, and Cu in every sediment core

Core	Pb		Zn		Cu	
	Highest concentration (mg/kg)	Depth (cm)	Highest concentration (mg/kg)	Depth (cm)	Highest concentration (mg/kg)	Depth (cm)
Core I	69.10	29.00	91.00	29.00	40.60	29.00
Core II	30.67	33.00	78.74	42.00	-	-
Core III	63.02	27.00	71.85	27.00	28.40	33.00
Core IV	57.85	40.00	78.02	27.00	27.59	40.00
Core V	49.86	42.00	84.60	42.00	-	-

Almost the concentration of Pb, Zn, and Cu in five cores (Table 4.2) had a lower concentration than the content of the same elements along Bangyai canal (Suteerasak and Bhongsuwan 2008). This is evidence verify that the source of polluted heavy metal at Saphan Hin possibly accumulated from the previous tin mines. Moreover, the collected heavy metal concentration was compared with a standard guideline in the world (SQGs), which is suitably applied for assessing the presence of heavy metal in marine sediment (Sharifuzzaman et al. 2016). This result clearly showed the situation of pollution at coastal Saphan Hin in Figure 4.1, 4.2, 4.3.

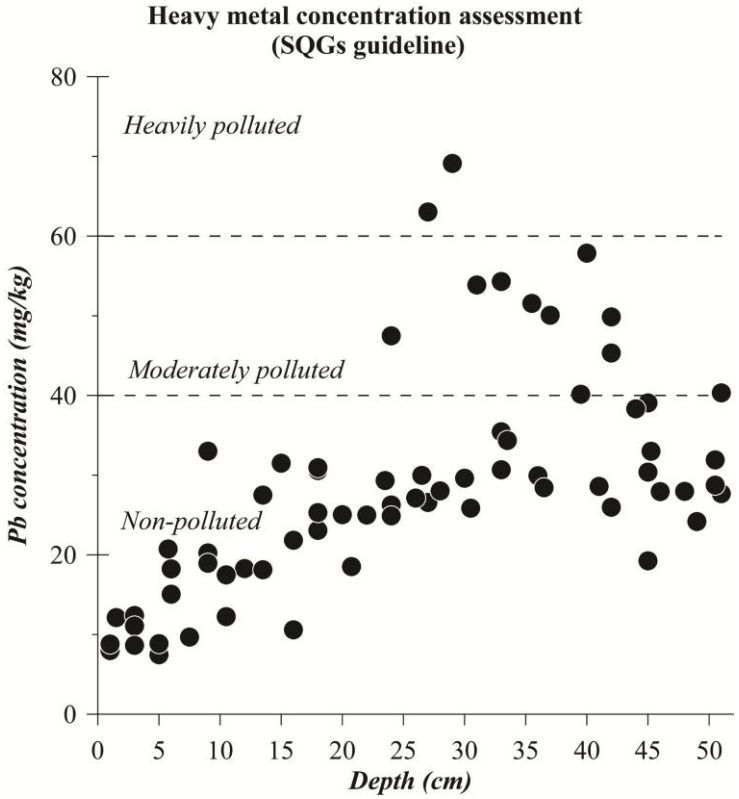

Figure 4.1 Pb concentration assessment by SQGs guideline

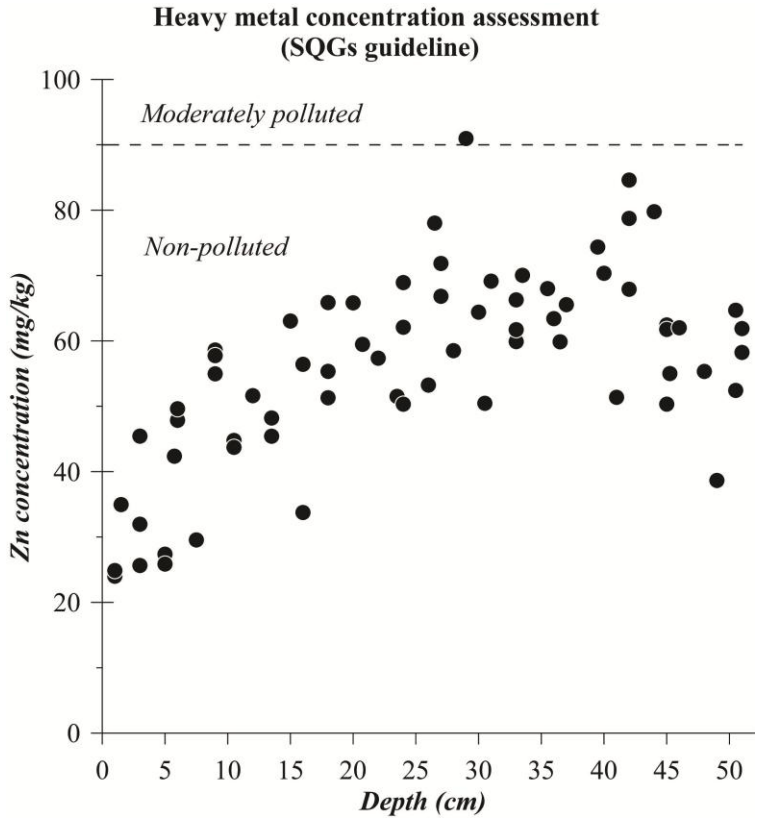

Figure 4.2 Zn concentration assessment by SQGs guideline

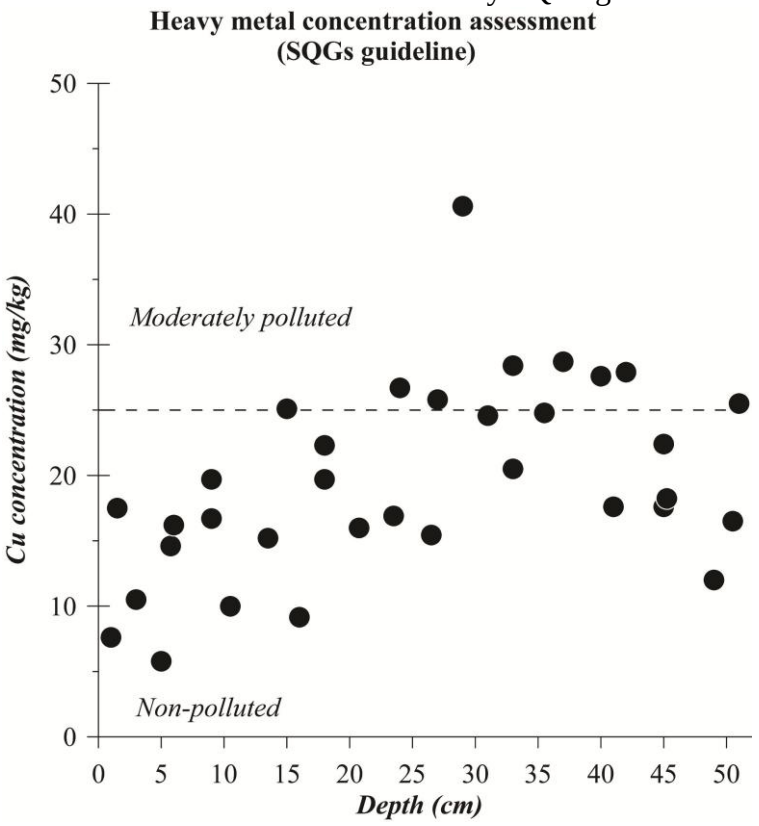

Figure 4.3 Cu concentration assessment by SQGs guideline

Generally, at Saphan Hin coast the contamination of heavy metal (Pb, Zn, and Cu) at moderate pollution to slightly heavy pollution. While Zn has only value at moderate contamination (at 29 cm in core I); Pb, Cu have amount value at moderate pollution (from 27 cm to 40 cm depth). Among all cores, core I gave the evidence to show that at depth 29 cm, level of contamination is the worst with 69.10 mg/kg in Pb and 90.96 mg/kg in Zn, 40.60 mg/kg in Cu. The highest concentrations at this location might result is located nearest to the estuary of core I. Besides, only Pb concentration of core II in five cores showed that unpolluted because the maximum value is under the standard level of SQGs with 30.67 mg/kg.

Cross sections were made from five cores (Figure 4.4 – Figure 4.8):

+ Cross section one includes core I, II, III

+ Cross section two includes core IV, V

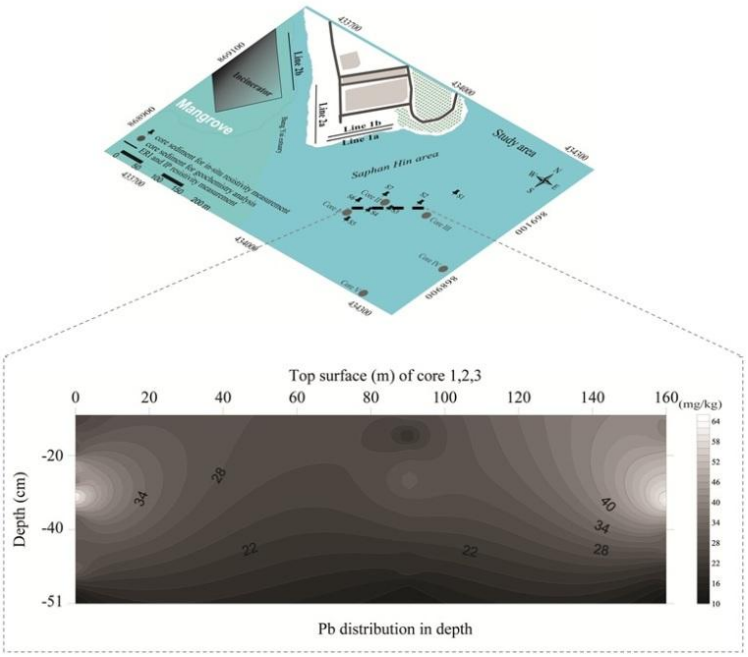

Figure 4.4 Cross section of Pb concentration (core I, II, III)

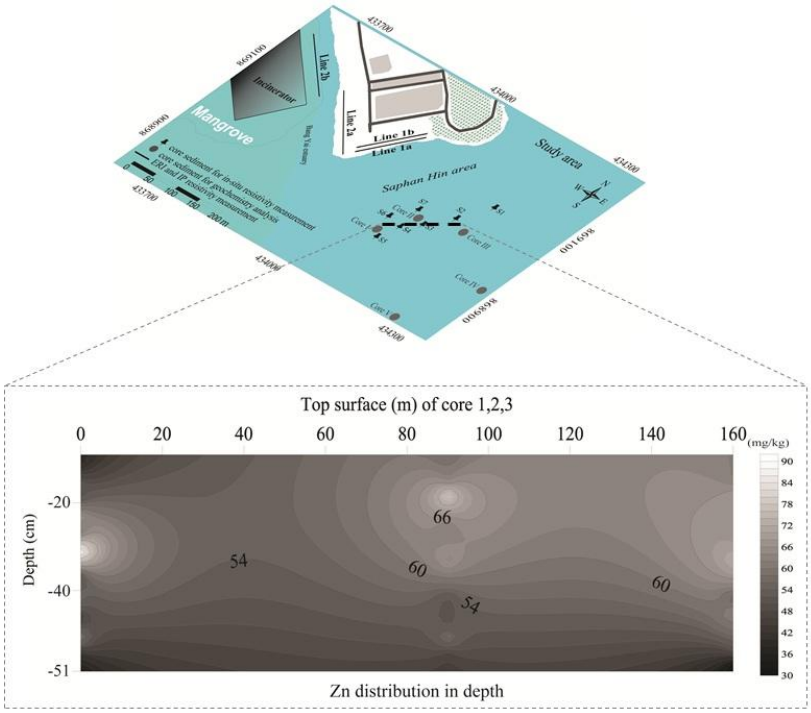

Figure 4.5 Cross section of Zn concentration (core I, II, III)

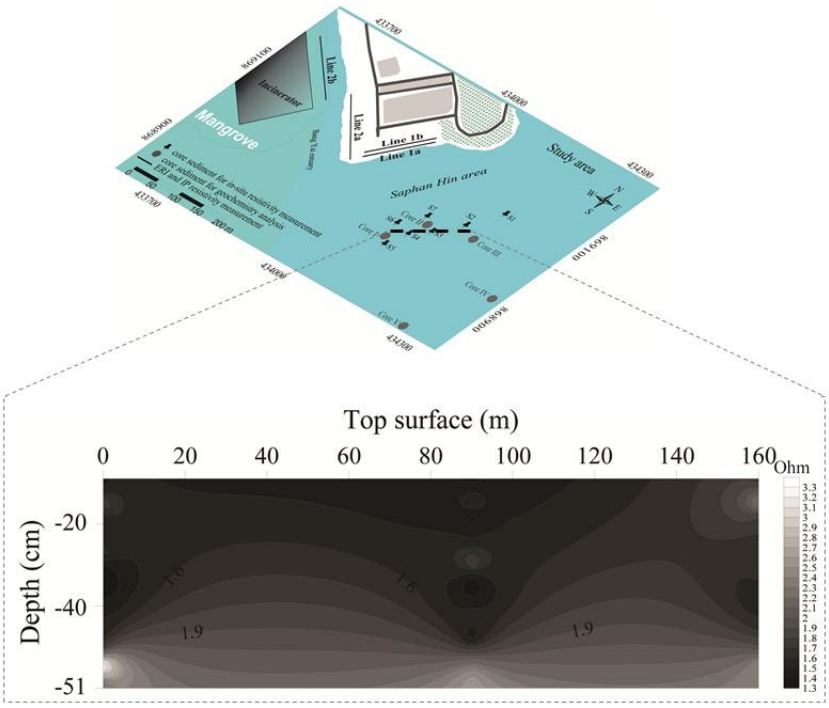

Figure 4.6 Cross section of resistivity value (core I, II, III)

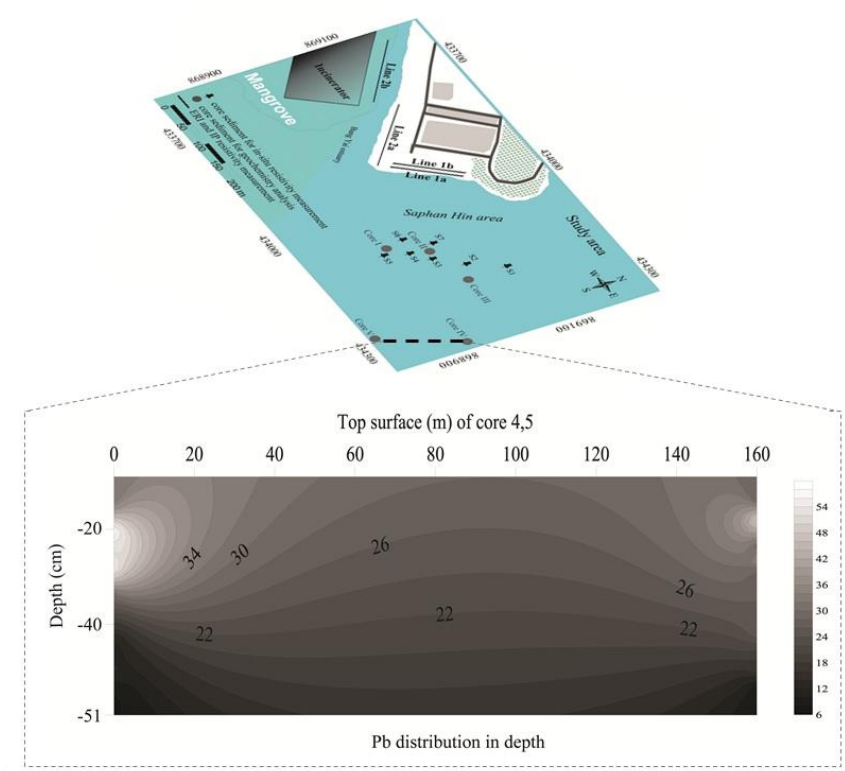

Figure 4.7 Cross section of Pb concentration (core IV, V)

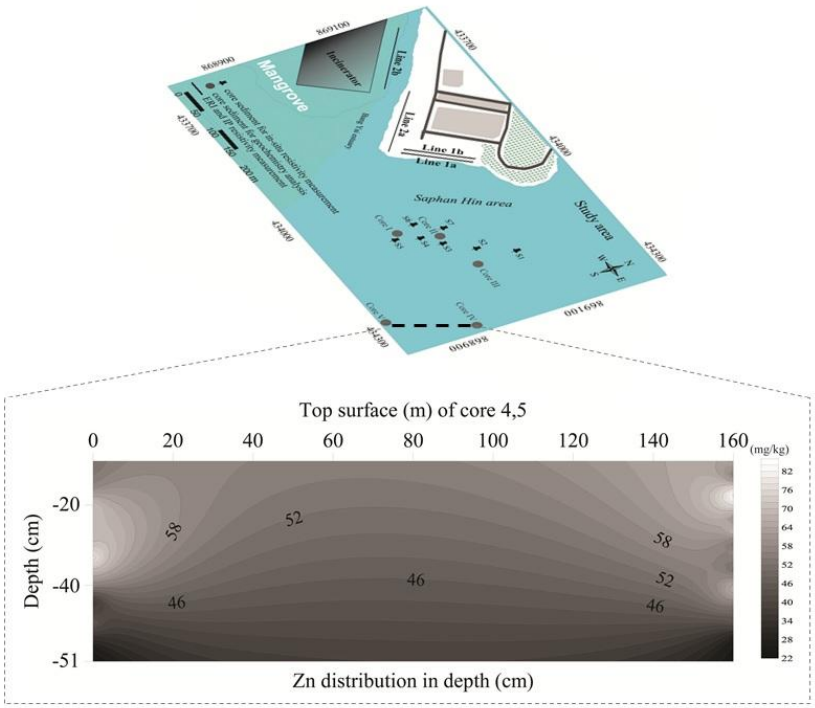

Figure 4.8 Cross section of Zn concentration (core IV, V)

The decrease of Pb, Zn concentration was shown clearly in two cross-section groups. Highest Pb concentration reduces from 69.11 mg/kg to around 58 mg/kg and the highest Zn concentration fall down from approximately 91 mg/kg to 72 mg/kg. Close with the sea, the concentration of Pb, Zn has a downward trend.

The cross-section contours of Pb, Zn are the interpretation of the data of heavy metal concentration in five cores as vertically and parallel to the seashore (North-East) as in Figure 4.4 to Figure 4.7. The results found that the accumulation of heavy metal concentration reduced according to the depth. Almost, the presence of moderate-heavy metal (Pb, Zn) pollution was sought from 10cm to 50 cm depth, (Figure 4.4) and at 30 cm (Figure 4.5). It is possibility shown that mining was a reason caused this contamination because the heavy metal contamination has increase tendency from the surface to deeper site (especially at 15-35 cm depth), the term mines closed in 1995. Suteerasak and Akkajit (2018) showed a similar result toward the accumulation of Pb, Zn and Cu in the sediment of BangYai canal when the concentration of heavy metal decrease from the top down to the bottom of a core. Hence, the close of tin explores mine significant reduce the dispersion of the amount of heavy metals at coastal Saphan Hin.

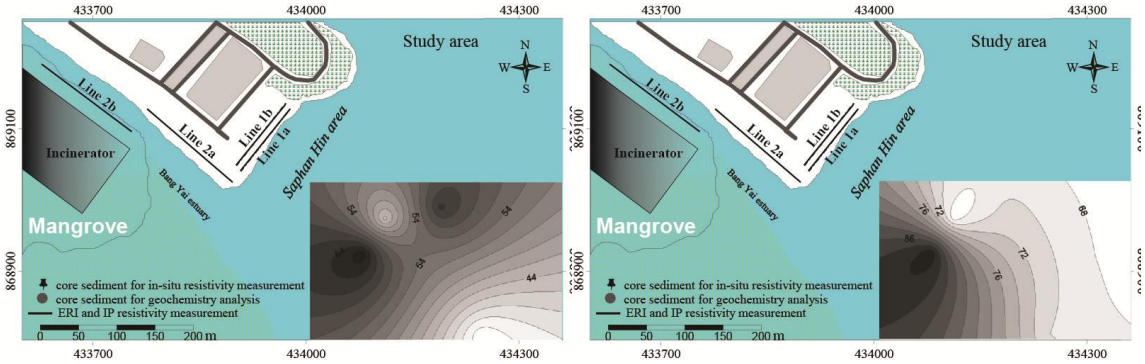

a) b)

Figure 4.9 Planar view of Pb and Zn distribution contour in the sediment at 29-33.5 cm depth (Puttiwongrak et al. 2019)

The highest concentration of Pb, Zn was found at the depth from 29 to 34 cm (Figure 4.9). According to the contour color in figure 4.9a reduction of Pb contamination levels at distances offshore were observed. Conversely, the shape contour of figure 4.9b presented the lower Zn concentration is far from the estuary.

On the other side, along Bangyai canal, there are no factories or any manufactories, these connect to illustration contours (lower heavy metal lever is distant from the estuarial area) can explain that the original heavy metal source comes from the mainland and human activities (weathering, domestic waste from incinerator).

4.1.2 Igeo, EF indexes

Igeo, EF are two indicators, which used to value the appearance and level of anthropogenic contaminate deposit on topsoil (Barbieri 2016). The two indexes also showed the level of contamination of sediment at Saphan Hin area.

Table 4.3 Igeo, EF values of Pb, Zn, and Cu

Core	**Igeo**			**EF**		
	Pb	**Zn**	**Cu**	**Pb**	**Zn**	**Cu**
Core I	-1.31	-1.78	0.22	2.07	1.49	5.99
	-0.53	-1.50	-0.04	2.80	1.43	3.94
	0.14	-1.03	0.39	2.51	1.12	3.00
	-0.13	-1.40	0.01	2.40	0.99	2.64
	0.03	-1.12	0.39	2.12	0.96	2.73
	-0.03	-1.22	0.17	1.96	0.86	2.27
	1.20	-0.40	1.44	2.39	0.79	2.80
	0.24	-1.00	0.45	2.25	0.95	2.60
	0.74	-0.87	0.93	2.39	0.78	2.74
	-0.07	-1.22	0.23	2.26	1.02	2.78
	0.02	-1.25	0.23	2.15	0.89	2.49
	-0.31	-1.63	-0.32	2.39	0.96	2.37
	-1.28	-1.40	-	3.34	3.06	-

Core	Igeo			EF		
	Pb	**Zn**	**Cu**	**Pb**	**Zn**	**Cu**
Core II	-0.99	-1.33	-	2.59	2.06	-
	-0.57	-1.06	-	2.47	1.76	-
	-0.71	-1.22	-	2.44	1.72	-
	-0.38	-1.23	-	1.88	1.05	-
	-0.19	-0.95	-	2.33	1.37	-
	-0.17	-0.84	-	2.57	1.62	-
	-0.02	-0.90	-	2.24	1.22	-
	0.03	-0.96	-	2.45	1.23	-
	0.00	-0.92	-	1.85	0.98	-
	-0.21	-0.61	-	1.76	1.33	-
	-0.64	-0.94	-	2.00	1.62	-
	-0.12	-1.04	-	1.70	0.90	-
Core III	-1.44	-1.91	-0.51	2.22	1.60	4.20
	-0.72	-1.27	0.11	1.85	1.26	3.28
	-0.66	-1.13	0.16	1.66	1.21	2.93
	0.07	-0.93	0.74	1.93	0.97	3.09
	0.04	-1.12	0.57	1.67	0.75	2.40
	0.66	-0.80	0.83	2.06	0.75	2.32
	1.07	-0.74	0.78	2.15	0.61	1.76
	0.86	-0.86	0.92	2.05	0.62	2.14
	0.60	-0.82	0.89	1.86	0.70	2.28

Core	Igeo			EF		
	Pb	**Zn**	**Cu**	**Pb**	**Zn**	**Cu**
	0.38	-0.96	0.58	1.62	0.64	1.86
	0.43	-0.96	0.76	1.67	0.64	2.11
Core IV	-1.91	-2.32	-0.98	1.96	1.48	3.74
	-2.01	-2.13	-1.38	1.77	1.62	2.73
	-1.29	-1.42	-0.59	1.72	1.58	2.81
	-1.50	-1.83	-0.71	1.57	1.25	2.72
	-0.70	-1.01	0.09	1.40	1.12	2.42
	0.00	-0.62	0.04	1.88	1.23	1.94
	0.84	-0.80	0.71	2.11	0.68	1.92
	0.78	-0.82	0.72	2.02	0.67	1.95
	0.95	-0.77	0.88	2.18	0.66	2.08
	0.14	-1.13	0.28	1.94	0.81	2.15
	0.09	-1.19	0.14	1.83	0.75	1.90
Core V	-1.77	-2.27	-	3.38	2.38	-
	-1.80	-2.23	-	3.36	2.49	-
	-1.76	-2.21	-	3.27	2.39	-
	-1.63	-2.02	-	2.83	2.16	-
	-0.78	-1.46	-	2.16	1.35	-
	-0.73	-1.32	-	1.86	1.23	-
	-0.46	-1.09	-	1.59	1.03	-
	-0.25	-0.87	-	1.54	1.00	-

Core	Igeo			EF		
	Pb	**Zn**	**Cu**	**Pb**	**Zn**	**Cu**
Core V	-0.26	-0.87	-	1.66	1.09	-
	-0.26	-1.07	-	1.71	0.98	-
	-0.27	-1.25	-	1.62	0.82	-
	-0.15	-1.17	-	1.55	0.76	-
	-0.10	-1.04	-	1.59	0.83	-
	-0.21	-1.25	-	1.57	0.77	-
	0.20	-0.78	-	1.62	0.82	-
	-0.08	-1.00	-	1.79	0.94	-
	0.42	-0.69	-	1.69	0.78	-
	0.73	-0.50	-	1.49	0.63	-
	0.35	-0.59	-	1.73	0.90	-
	-0.10	-0.95	-	1.84	1.02	-
	-0.10	-1.12	-	1.89	0.93	-
	-0.06	-0.89	-	1.45	0.82	-

In Figure 4.10, the heavy mental assessments by using Igeo index show clearly result in three analyzed elements. Igeo of Zn is lowest with all Igeo values in five cores is smaller 0, these show the absence of Zn contamination at research place. But almost Igeo value of Pb and Cu is the range of minor polluted to moderately polluted ($0<Igeo<1.5$) aside from a few points under 0 (no pollution signal). Generally, Igeo value of Pb and Cu are indicated worse pollution than of Zn.

By computing another index (EF), the EF assessment result shows a similar result compare with Igeo index. Content of Zn still holds the lowest contamination level with majority points at no enrichment and minor enrichment threshold. EF index of Cu is in minor and moderate enrichment except for a point at

significant enrichment. Pb values were in the extent from minor to moderate enrichment. Again, EF index confirmed for Igeo result that the contamination of Zn in nature is better than of Pb and Cu.

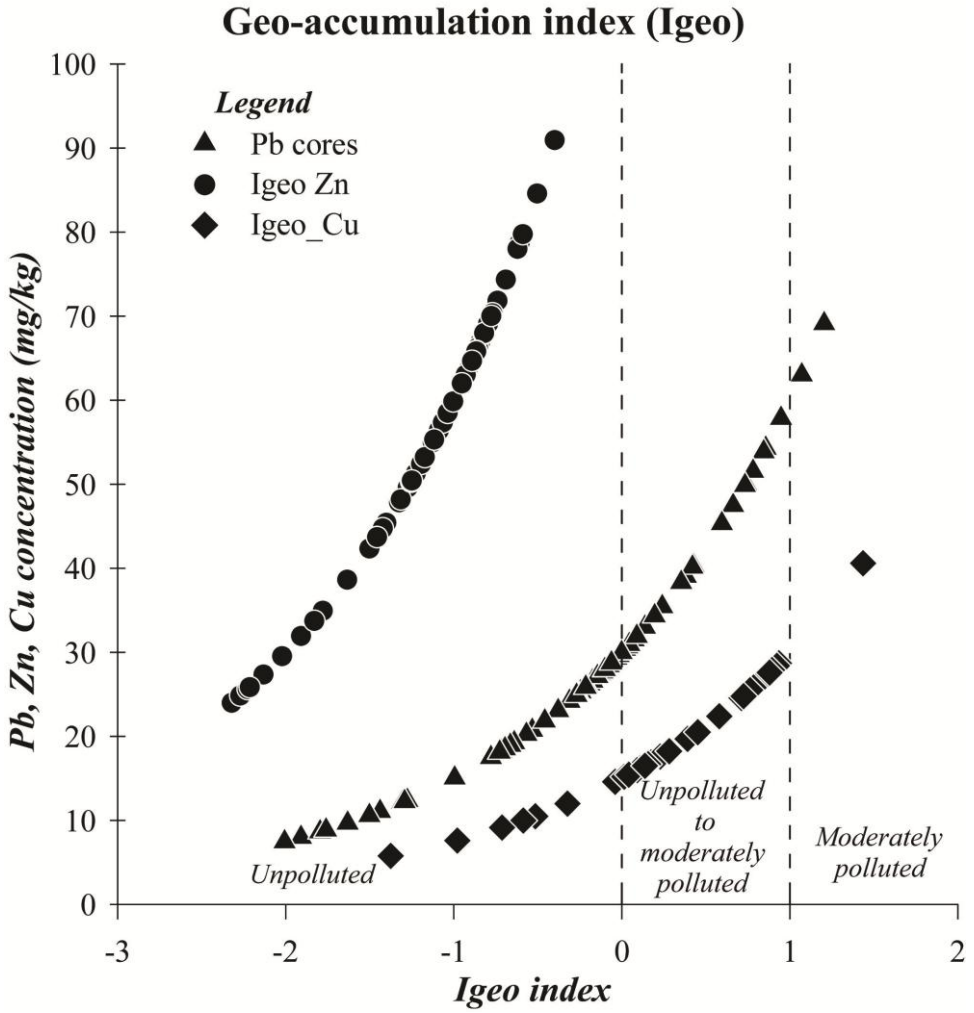

Figure 4.10 Pollution assessment of Pb and Zn by Igeo index

Cu has the accumulation index is highest with 1.4 and Zn has lowest Igeo with -2.3. The result of Zn depicted that the accumulation of Zn in sediment is no pollution and Cu, Pb is at moderately polluted ($0 < Igeo \leq 2$)

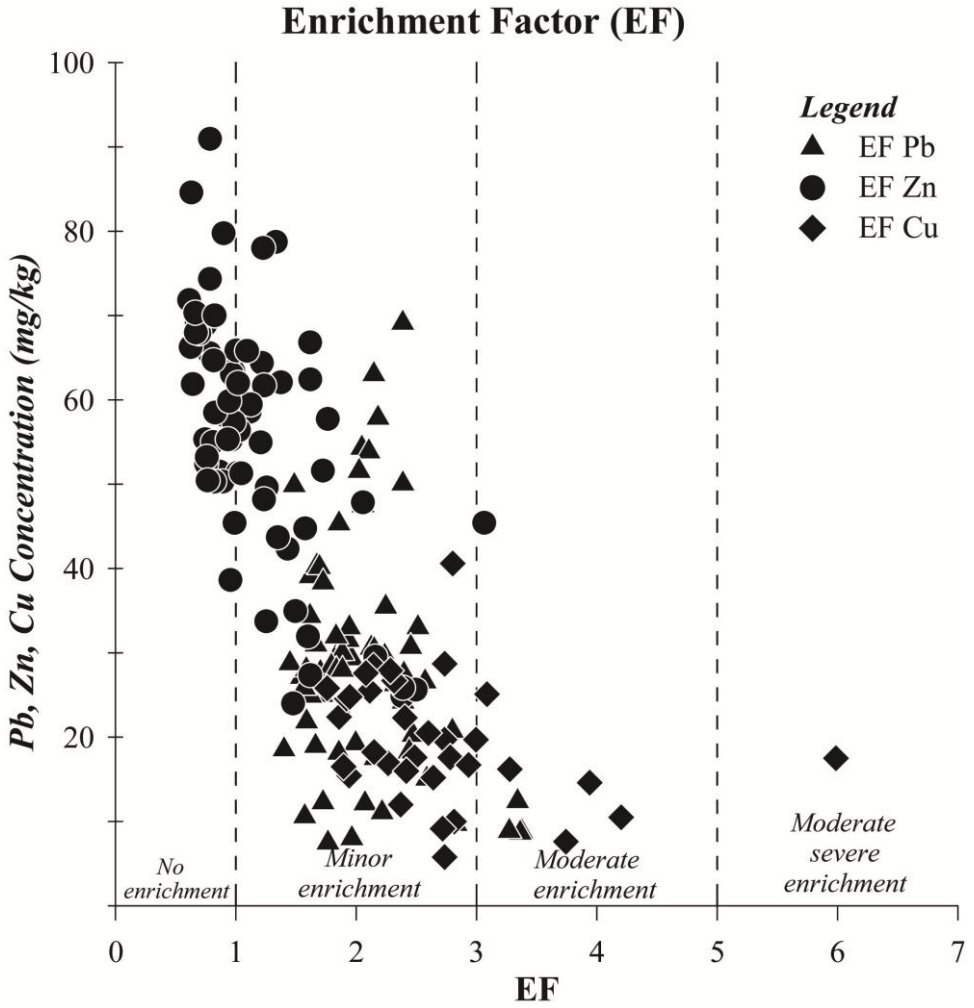

Figure 4.11 Pollution assessment of Pb and Zn by EF index

The enrichment factor of Zn in sediment is relatively small at no enrichment level and a few points with minor enrichment (EF starts from 0.6 to 3). Pb holds the second lowest EF with level from 1.4 to 3.3. Finally, Cu is an element has a serious situation with the rank of enrichment factor from 1,76 to 6 with 1 point stay in moderate-severe enrichment. If $0 \leq EF \leq 1.5$ demonstrates that accumulation of heavy metal is caused by the natural weathering process, $EF > 1.5$ shows that accumulation of heavy metals is made by other sources as anthropogenic activities (Barbieri 2016). At study area, therefore, the presence of heavy metal results in not only crust weathering but also from people (such as urban waste, mining waste…).

4.1.3 Coefficient between heavy metal

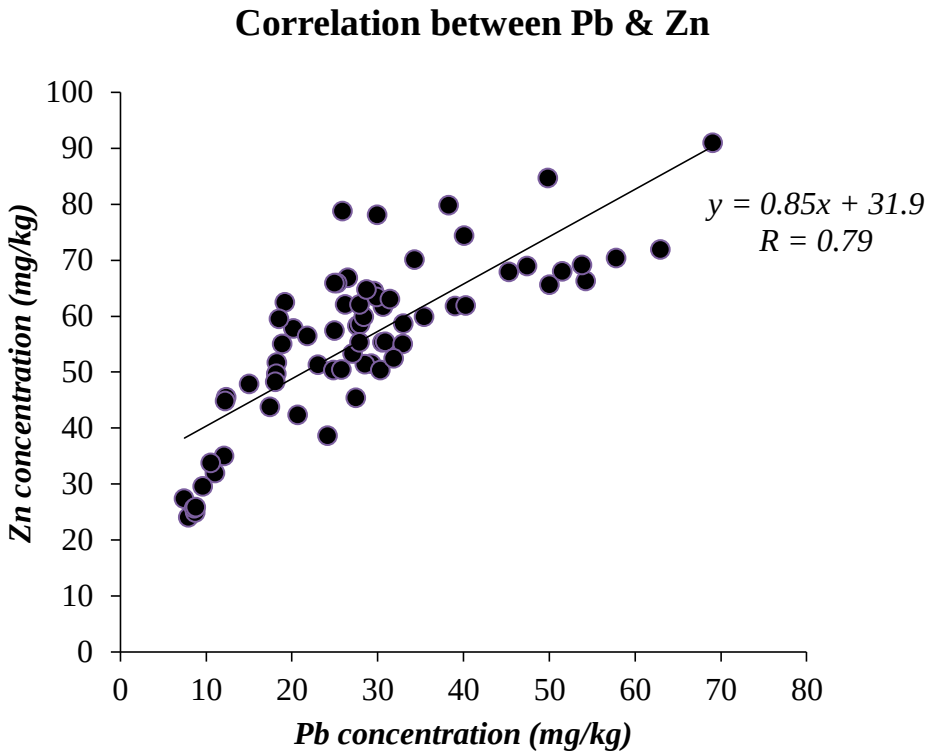

Figure 4.12 Correlation between Pb and Zn concentration

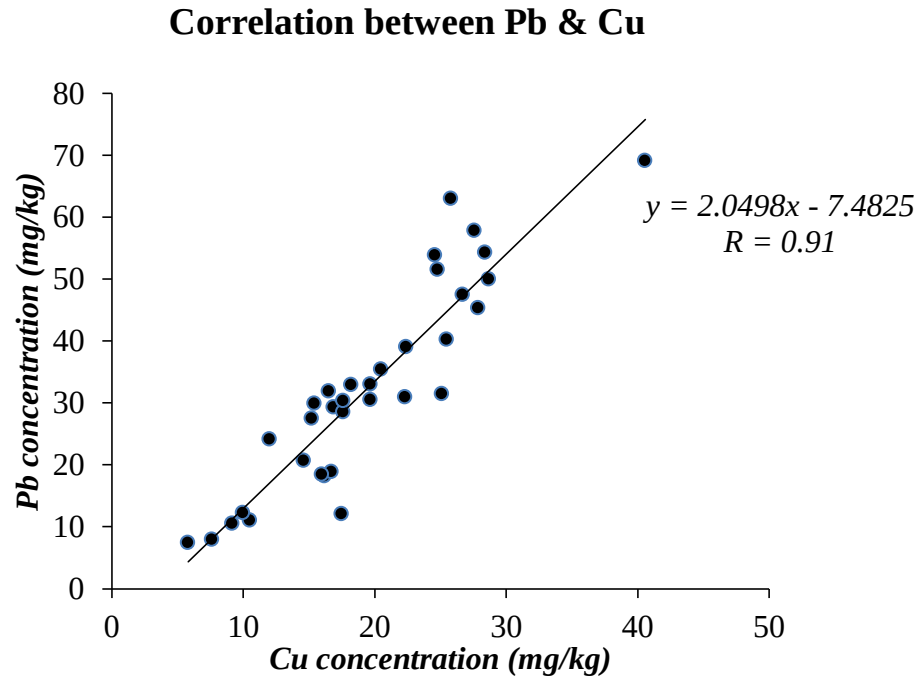

Figure 4.13 Correlation between Pb and Cu concentration

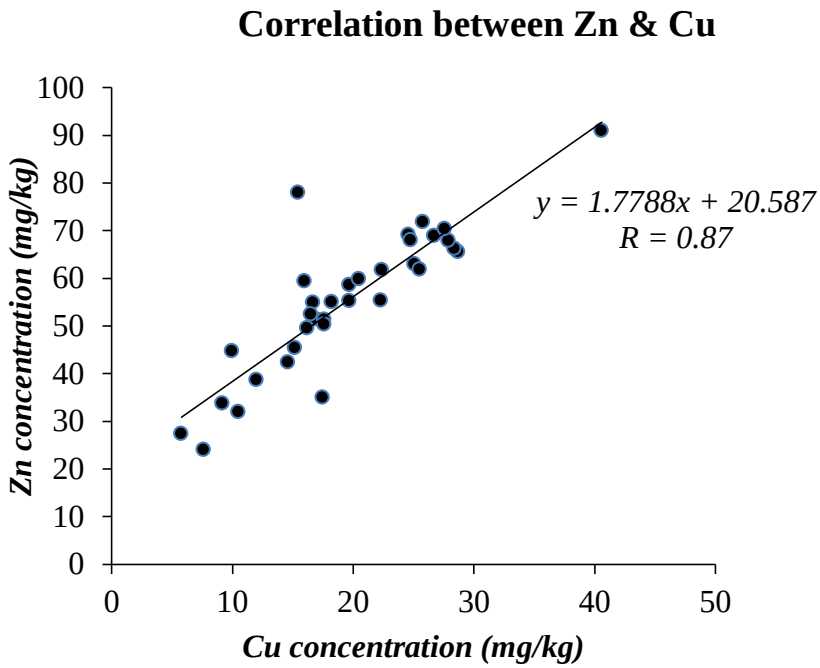

Figure 4.14 Correlation between Zn and Cu concentration

Pearson correlation was used to value the relationship between Pb, Zn, and Cu. Commonly, these three elements have a relatively good connection. The best value belongs to Pb and Cu with r = 0.91 (Very strong correlation), continuously Zn and Cu has a significant correlation (with r = 0.87) and finally is a relationship of Pb and Zn with r = 0.79. This result is a supported association of three heavy metals in nature.

4.1.4 Coefficient between resistivity value and heavy metal concentration

Heavy metal concentration got from boreholes combined with in-situ testing resistivity value took in the vicinity area was categorized into three groups (the first group: with S4-6 and core I, The second group: S3-4 and S7 with Core II, and the third group: S1-2 with Core III). The correlation between metal concentration (Zn and Pb) and in-situ resistivity value was qualitatively illustrated in figure 4.15, below:

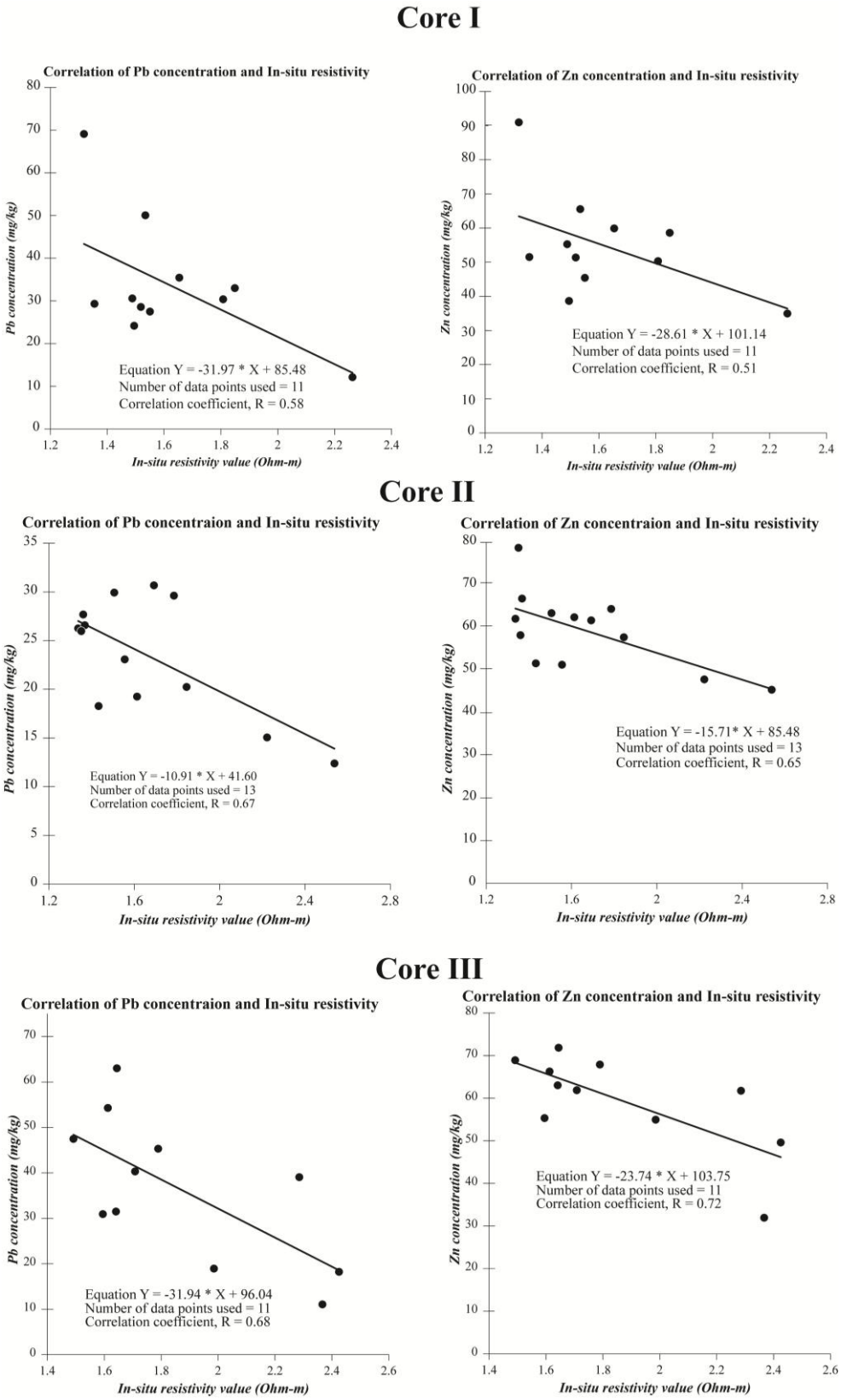

Figure 4.15 Relationship of Zn, Pb concentrations measured by CA and in-situ resistivity (core I, II, III)

Crossplot of correlation between the value of Zn, Pb concentrations and In-situ resistivity depicted that the increased value of Pb and Zn in all cores (core I, core II and core III) is opposite with the decreasing trend of resistivity in sample group (S1-S7). The Correlation coefficient (r) between Zn (core I, core II, core III) and in-situ resistivity (three groups) were -0.58, -0.65, and -0.72. Similarly, the correlation coefficients between Pb and in-situ resistivity were -0.51, -0.67, and -0.68. Despite r did not mean that the correlation between heavy metal concentration (Zn, Pb) and resistivity value were a strong correlation, but all r values are negative correlations (downhill linear lines), also proved that Pb and Zn and resistivity value are reversible factors. However, at the first core and Group I, the r value is a little bit low with (r=0.58 and r=0.51 toward Pb and Zn and in-situ resistivity, respectively) could be affected by the interference of seawater and water from Bangyai canal or the appearance of other minor heavy metals contaminated

Besides, the relationships between heavy metal (Pb, Zn) and resistivity were confirmed with statistical significance level, P-value and briefly in table 4.4

Table 4.4 Pearson's product-moment correlation of core I, II, II and in-situ resistivity

Statistical parameter	**Core I**		**Core II**		**Core III**	
	Zn and *ρ*	**Pb and *ρ***	**Zn and *ρ***	**Pb and *ρ***	**Zn and *ρ***	**Pb and *ρ***
Variable X	Resistivity	Resistivity	Resistivity	Resistivity	Resistivity	Resistivity
Variable Y	Zn	Pb	Zn	Pb	Zn	Pb
Correlation coefficient, r	-0.51	-0.58	-0.65	-0.68	-0.72	-0.68
Significance level, P-value	0.10	0.06	0.02	0.01	0.01	0.02
95% Confidence interval for r	-0.85 to 0.13	-0.87 to 0.03	-0.88 to -0.15	-0.89 to -0.19	-0.92 to -0.21	-0.91 to -0.13

Base on the significance level, P-value ($P<0.05$) that heavy metal concentration of Zn, Pb has a negative correlation with resistivity value (R) of the beneath of the surface in the research expense. While heavy metal concentration in the

subsurface is high, the resistivity value is low (< 2.40 Ohm-m). This relationship assumed that a resistivity value is a good indicator in seeking heavy metal contamination in nature. This is a significant result in research because normally, heavy metal contamination uses chemical analysis, which demands high technique and cost in sample size to achieve accurate results. So these results are very significant in support using ERI method to find the heavy metal levels.

4.1.5 Find the empirical value for resistivity value

Illustration of trend curves of correlations between resistivity and heavy metal contaminations (Pb and Zn) (in Figure 4.15) can be a background in finding threshold value for heavy metal. Not only calculated r-value but every core was set up a linear equation between heavy metal concentration and resistivity. To assess whether the soil is contaminated or not, SQGS guideline was applied as a standard with 90 mg/kg for Zn and 40 mg/kg for Pb because following the SQGS guideline, at Pb≥40 and Zn≥90 that site is considered as a polluted zone. After that, these values were used to find resistivity value. The results show in Table 4.5

Table 4.5 Empirical resistivity value calculation base on linear equation

Core I	
Pb - resistivity value (Ohm-m)	Zn - resistivity value (Ohm-m)
y = -31.96x + 85.48 |x| = 1.42	y = -28.61x + 101.14 |x| = 0.39
Core II	
Pb - resistivity value(Ohm-m)	Zn - resistivity value (Ohm-m)
y = -10.91 * x + 41.60 |x| = 0.15	y = -15.71 * x + 85.48 |x| = 0.29

Core III	
Pb - resistivity value(Ohm-m)	Zn - resistivity value (Ohm-m)
y = -31.94 * x + 96.04 |x| = 1.75	y = 23.74 * x + 103.75 |x| = 0.58
Average = 0.76 Ohm-m	

The resistivity values mention the contamination of Pb, Zn are 1.42 Ohm-m, 0.39 Ohm-m, 0.15 Ohm-m, 0.29 Ohm-m, 1.75 Ohm-m, 0.58 Ohm-m. The resistivity of x in equation with Pb and Zn respectively: 1.42 Ohm-m, 0.15 Ohm-m, 1.75 Ohm-m (with Pb) and 0.39 Ohm-m, 0.29 Ohm-m, 0.58 Ohm-m (with Zn). Sample standard deviation of resistivity value:

$$\sigma = \sqrt{\frac{1}{N-1}\sum_{i=1}^{N}(\overline{x_i} - \bar{x})^2}$$

While:

$\overline{x_i}$: Value of the ith in data set

$\bar{x}$: The mean value of data set

N: the number of data

So standard deviation of resistivity value:

$$\sigma = \sqrt{\frac{1}{6-1}[(1.42-0.76)^2 + (0.39-0.76)^2 + (0.15-0.76)^2 + (0.29-0.76)^2 + (1.75-0.76)^2 + (0.58-0.76)^2]}$$

$$\sigma = 0.65 \text{ (Ohm-m)}$$

Core II has the lowest resistivity value with (Resistivity of Pb, Zn are 0.15 Ohm-m and 0.29 Ohm-m, respectively) while the highest resistivity value is 1.75 Ohm-m (in core III). Additionally, with average value is 0.76 Ohm-m and sample standard deviation is 0.65 Ohm-m, it is clear that the resistivity value of heavy metal elements (Pb, Zn) in this research has a large variation start from 0.11 Ohm-m to 1.41 Ohm-m. In ERI method, nevertheless, it is difficult to give a conclusion about what is the exact value of resistivity, which might perfectly indicate the heavy metal accumulation at a zone was over standard. Associated with tried versions in EarthImage 2D software, 1 Ohm-m is seemed to be the nearest the average resistivity

value, apposite with a gap of calculated sample standard deviation and also showing clearly 2D inversions about polluted zone, hence the resistivity value is smaller than 1 Ohm-m was chosen to classify the potential contamination of heavy metals in next ERI method at this study area.

4.2. Geophysics resistivity value results

The find heavy metal zone was done base on two factors: resistivity and IP value. Basically, low resistivity is mentioned as a contaminated zone or sea water instrument because they comprise ions and conductive molecules (Plata and Rubio 2004). Otherwise, the low resistivity value can also infer as the seawater intrusion in the coastal zone. Abundant sodium chloride (NaCl) in high concentrations levels of seawater often has low low resistivity (Kura et al. 2014). However, IP value is the main element to distinct two problems. For instance, low resistivity (6 to 33 Ohm-m) and IP smaller than 4ms, it showed the contaminated area of leachate plume; but, IP ranges from 8 to 13 ms, this is rich clay zone, or if IP start from 16 ms to 40 ms, it is not clay but a distributed organic waste. Basically, the resistivity is less than 10 Ohm-m is remarked as low resistivity of contamination zone or leachate plume. At Seri Petaling, State of Selangor, Malaysia, for instance, the authors assumed that: a leachate zone has resistivity lower than 2.99 Ohm-m, a sand saturate has resistivity from 4.95-5.05 Ohm-m, a contamination with leachate has resistivity between 3.50-4 Ohm-m, finally, the resistivity of a freshwater saturated with leachate ranges from around 6.03-7.15 Ohm-m (Ahmed and Sulaiman 2001); In Portugal, the polluted location of sand was shown with low resistivity (<45 Ohm-m) and high IP (>8 ms) (Srigutomo et al. 2016). Srigutomo et al (2016) also explored manganese prospective zones with combination results of resistivity and IP value with lower than 5 Ohm-m and higher than 10 ms, respectively. Combine with the previous researches and the empirical value was calculated in part 3.3, a scale for resistivity was established with resistivity is smaller or equal 1 Ohm-m is regarded as a signal of the heavy metal zone.

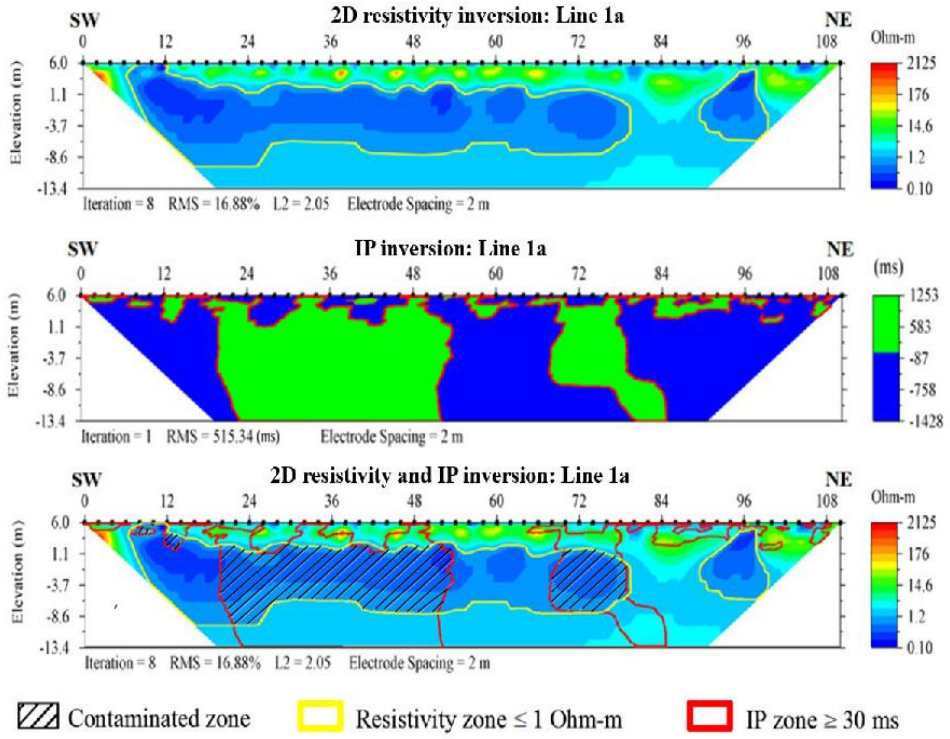

Figure 4.16 Contamination zone in 2D ERI interpretation - Line 1a (Puttiwongrak et al. 2019)

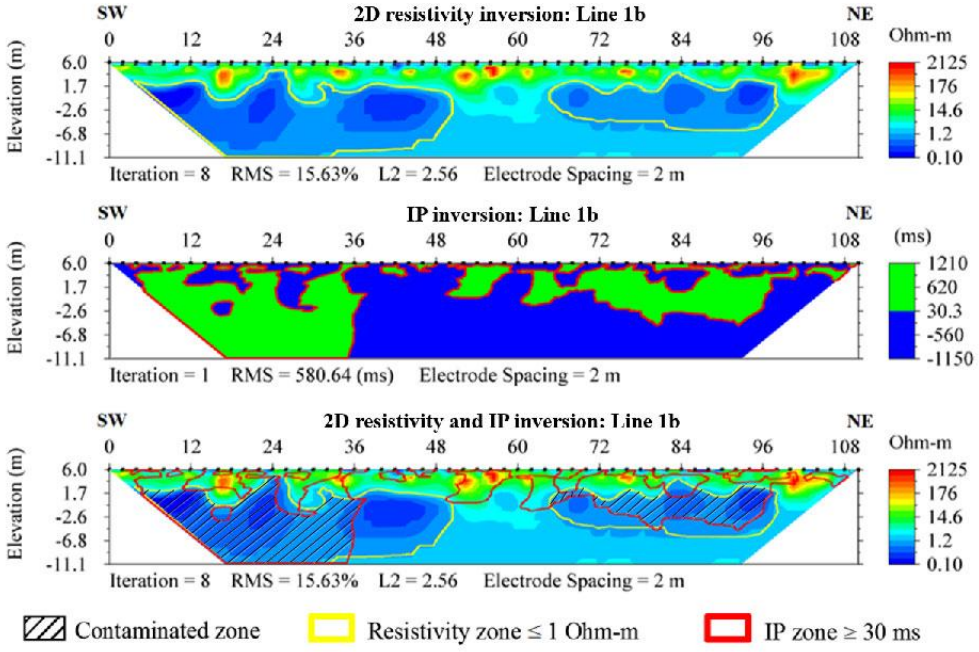

Figure 4.17 Contamination zone in 2D ERI interpretation - Line 1b (Puttiwongrak et al. 2019)

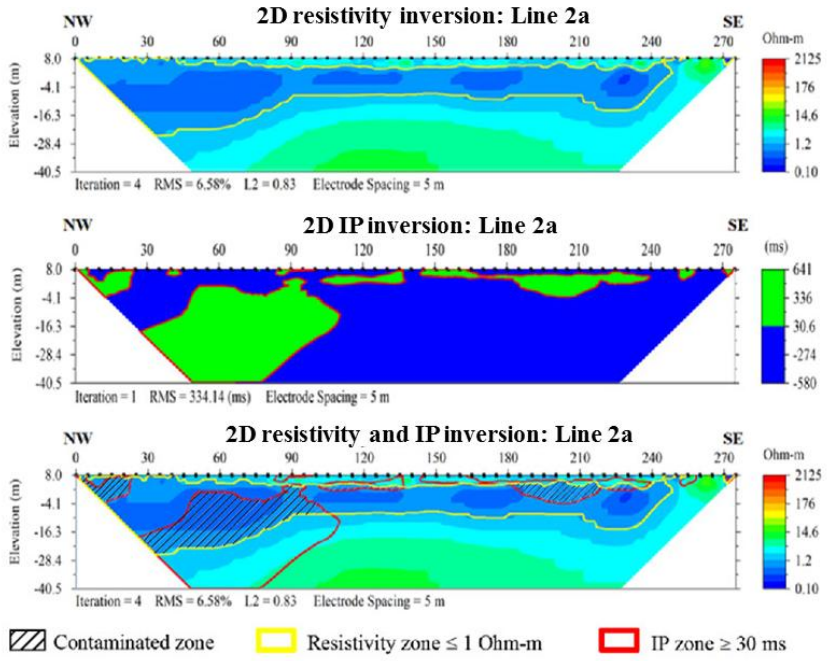

Figure 4.18 Contamination zone in 2D ERI interpretation - Line 2a (Puttiwongrak et al. 2019)

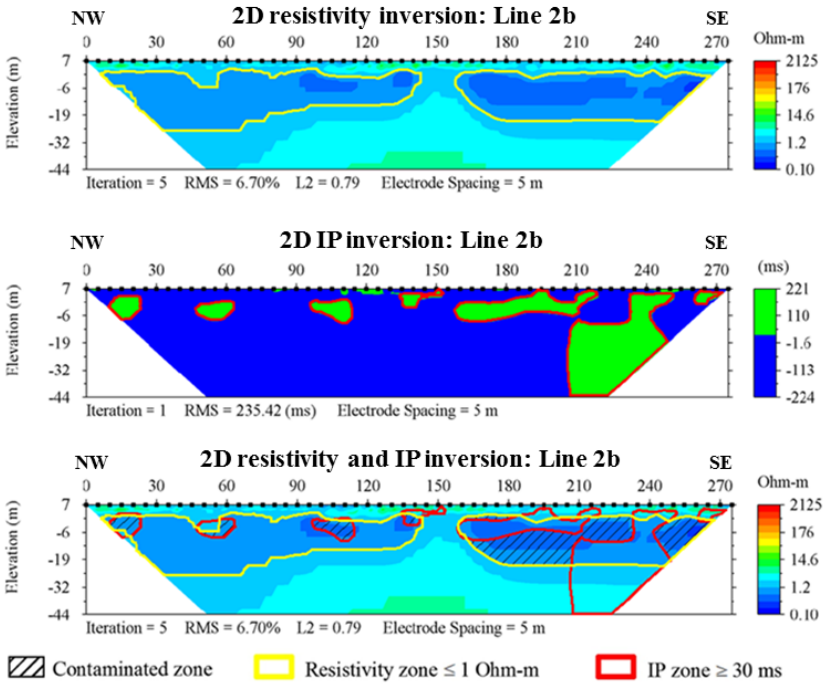

Figure 4.19 Contamination zone in 2D ERI interpretation - Line 2b (Puttiwongrak et al. 2019)

In four figures (Figure 4.16 – 4.19), at the range depth from 2 m to -11 m MASL of both line 1and line 2, the presence of underground contaminated zones was demonstrated through the special feature of 2D ERI imaging (including resistivity and IP). In four figure, the the values of RMS show relatively good value with RMS of Line 1a, Line 1b, Line 2a, and line 2b are 16.88%, 15.63%, 6.58%, 6.7%, respectively. While the contamination zone of line 1a, line 1b locates down to the bottom site of the figure; at line 2a, 2b, the contaminated zone appears shallow surface zone (Figure 4.18; 4.19). Because Line 1a is nearer to the sea than Line 2a, it might be the cause lead to the low resistivity zone in Line 1a is bigger than Line 2a. Whether the low resistivity is the result of seawater instrument or not because low resistivity is a signal of this phenomenon (Kura et al. 2014). If it is difficult to distinguish the seawater intrusion and heavy metal contamination with the only resistivity result, Chargeability (IP) will play a significant role in this problem. The high level of contamination caused by heavy metal often has high chargeability ($\geq$ 30 ms) (Abdullahi et al. 2011). The high chargeability zone clearly depicted in every second picture of Figure 4.16, 4.17, 4.18 and 4.19. In the contaminated soil, the ion concentration increase is caused by the high concentration of heavy metal, this will make IP value will become more powerful in the contaminated soil (Uchegbulam and Ayolabi 2014). Otherwise, grain size, the material of soil also effect to the chargeability value, but the determination of how type of mineral affects to the only chargeability is not normally used (Jones 2007). The interpretation results for the contaminated zone in this research was done base on only the combination of ERI and IP inversion and without other effects. In every figure (Figure 4.16, 4.17, 4.18, 4.19) comprises three small pictures inside with different meaning. The first one is 2D resistivity inversion; the second one is IP inversion and the thirst one is overlaying images between ERI and IP inversion. The overlaying zone of ERI and IP is interpreted as a contaminated zone. However, there is one disadvantage point in this method is unable accurately defined the type and level contamination of research area. This is the reason is why CA method is very necessary to support this comprehensive research.

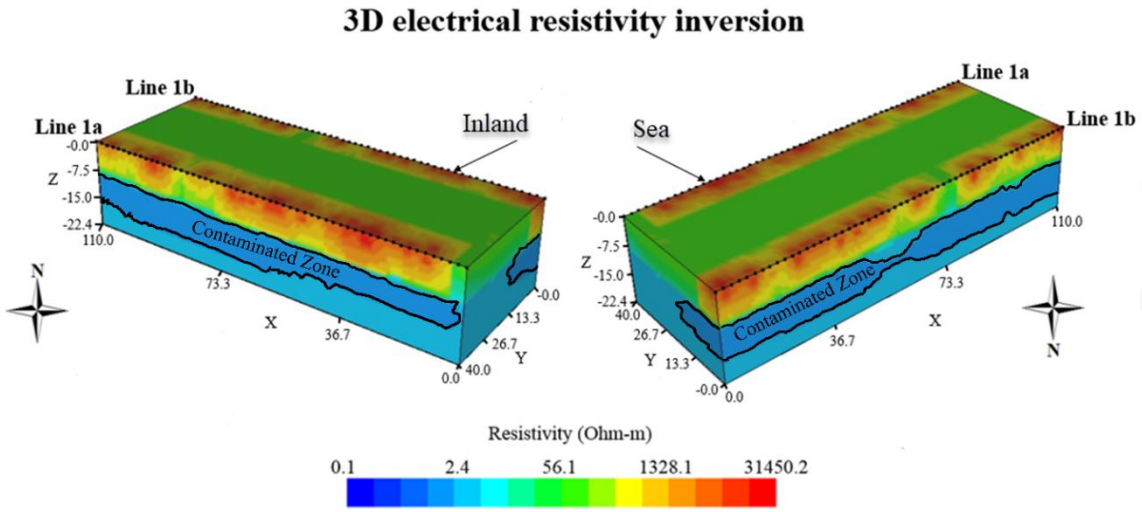

Figure 4.20 3D ERI inversion results between Line 1a and 1b (Puttiwongrak et al. 2019)

In a wider perspective comparison to 2D ERI, 3D ERI can support to estimate the movement of undersurface conformation of contamination zone as in Figure 4.20, 3D ERI results are the connection of line 1a and line 1b, where closes to the sea. Results from the 3D ERI provide additional information indicating that the contaminated zone is more highly concentrated in the bottom part of the coastal area. The 3D ERI shows a layer of materials with low resistivity values (<2.4 Ohm-m) as the pocket of resistivity volume, representing a contaminated zone in the study area.

CHAPTER 5
CONCLUSIONS

In this research, the investigation of contamination problem of a Saphan Hin coast was completed by applying simultaneously two methods: Geoelectrical method (ERI/IP) and geochemical analysis (analysis concentration, compute Igeo and EF indexes). Besides, the study using a few heavy metal concentration standards to assess the level of pollution of the research area. Application geo-chemical method (measure heavy concentration, compute Igeo, EF index) gave a similar result about the pollution of the research area. Generally, at Saphan Hin coast, the contamination of Pb, Cu, Zn is at moderate to heavily level. By interpreting four profiles of geo-electrical surveys, 5 soil cores collected for chemical analysis with three metal (Pb, Zn, Cu), seven soil cores for checking electrical conductivity value in a large coastal area (around 500 m^2) could ascertain the situation and distribution zone of the contamination at coastal Saphan Hin. Maximum polluted levels of Pb, Zn, Cu were determined in sediment at a range from 10 to 50 cm respectively are 667.40 mg/kg, 91.20 mg/kg and 40.60 mg/kg. This place is quite far from the land (several hundred meters), the zone is highest Pb, Zn, Cu concentration was found at a maximum depth of around 29-33 cm. Value of EF index and metal concentration measurement could help to establish the main reason was caused by anthropogenic activity (the previous tin mining in the past) because contamination could not find on the surface layer (from 0-10 cm). In the other hand, a combination between resistivity value and heavy metal concentration of (Pb, Zn) clarified the good result relationship of them to assert that ERI method can instead of geochemical toward the work finding the source of contamination of heavy metal and since then the cost for taking core sample and geochemical analysis can be significantly decreased. ERI indicated the layer of heavy metal contamination zone often is in 1.5 m MASL reduce to -11 m MASL in Figure 4.16 – Figure 4.19. The estuarial areas at beginning line 1a and line 1b have contamination area bigger than the further place.

The combination of ERI and Geochemical methods to assess level contamination of heavy metal in this research built a new way in using ERI method

replace for Geochemical to find heavy metal in nature. Nevertheless, every study area needs to set up a threshold for the corresponding resistivity to find out the exactly heavy metal zone. Connecting muti-mornitoring methods was evaluated level and zone the contamination of heavy metal concentration in the subsoil at Saphan Hin coast in Phuket Island. The results intents to protect not only the environment but also people health by toxic of a few heavy metals (as Pb, Zn, and Cu) which seemed as a consequence of exploring mineral mines, thenceforth, enhancing the consideration and change of communities in remaining green environment.

Heavy metal accumulation might bring many dangerous problems for human, organisms and the ecosystem if it is over the standard level. Although geochemical analyses are a method with high accurate in heavy metals accumulation assessment, this is a costly and invasive method. The result of this study suggests that the government or environment department should extend the investigation scope to seek for the source of pollution, especially toward Bangyai canal where provide the water to Saphan Hin. Otherwise, setting the threshold for resistivity value, which keeps the information of heavy metal opened a new approach to check the contamination accumulation of an area with ERI and IP methods. Taking borehole to check the heavy metal accumulation at the polluted sites is necessary to confirm the result. If the contamination zone, which was defined by the ERI method is the same with results in borehole sample, formation an early warning system for an area by using ERI and IP is completely possible.

REFERENCES

Abdullahi, N. K., Osazuwa, I. B., Sule, P. O. (2011). "Application of integrated geophysical techniques in the investigation of groundwater contamination: A case study of municipal solid waste leachate." *OJAS.*, 4(1), 7-25.

Ahmed, A. M., Sulaiman, W. N. (2001). "Evaluation of groundwater and soil pollution in a landfill area using electrical resistivity value is imaging survey." *Environ. Manag.*, 28(5), 655-63. doi:10.1007/s002670010250

Akkajit, P., Jaileak, K., Suteersak, T., Prueksakorn, K. (2017). "Assessment of Heavy Metals in Sediment at Saphan Hin, Phuket." In: Paper resistivity evaluated at *3rd rd International Conference of Low Carbon Asia and Beyond, Bangkok, Thailand.*

Anomohanran, O. (2018). "Hydrogeophysical and hydrogeological investigations of groundwater resources in Delta Central, Nigeria." *JTUSCI.*, 9(1), 57-68. doi:10.1016/j.jtusci.2014.06.003

Authman, M. M., Zaki, M. S., Khallaf, E. A., Abbas, H. H. (2015). "Use of fish as bio-indicator of the effects of heavy metals pollution." *J. Aquac. Res. Development*., 6(4), 1-13.

Ayangbenro, A. S and Babalola, O. O. (2017). "A New Strategy for Heavy Metal Polluted Environments: A Review of Microbial Biosorbents." *Int. J. Environ. Res. Public. Health.*, 14(1), 94.

Barbieri, M. (2016). "The Importance of Enrichment Factor (EF) and Geoaccumulation Index (Igeo) to Evaluate the Soil Contamination." *J. Geol. Geophys.*, 5(1), 1-4. doi:10.4172/2381-8719.1000237.

Bayram, Ü., Maraşlı, N. (2018). "Thermal conductivity and electrical resistivity dependences on growth rate in the directionally solidified Al-CuNi eutectic alloy." *J. Alloy. Comp.*, 753, 695-702

Beliles, R. P (1994). Tin. In: Clayton GD, Clayton FE, eds. *Patty's industrial hygiene and toxicology*, 4th ed. Vol. 2. New York, NY, John Wiley, 2258–2276.

Bernard, C., Colin, J. R., Anne, L. D. D. (1997). "Estimation of the hazard of landfills through toxicity testing of leachates." *Chemosphere*., 35(11), 2783-2796.

Bichet, V., Grisey, E., and Aleya. L. (2016). "Spatial characterization of leachate plume using electrical resistivity tomography in a landfill composed of old and new cells (Belfort, France)." *Eng. Geol.*, 211, 61-73. doi:10.1016/j.enggeo.2016.06.026

Bing, H., Wu, Y., Sun, Z. and Yao, S. (2011). "Historical trends of heavy metal contamination and their sources in lacustrine sediment from Xijiu Lake, Taihu Lake Catchment, China." *JES.*, 23(10), 1671-1678. doi:https://doi.org/10.1016/S1001-0742(10)60593-1

Brown, G., Buravas, S., Charaljavanaphet, J., Jalichandra, N., Johnston, W., Sresistivity valuethaputra, V. and Taylao, G. (1951). "Geologic Reconnaissance of the Mineral Deposits of Thailand."

Budavari, S. (2001). "The Merck index. An encyclopedia of chemicals, drugs, and biological." 13th ed. *Whitehouse Station*, NJ, Merck and Co., Inc

Climate. (n.d.). Retrieved from https://www.phuket.net/visit-phuket/about/info/climate/ (accessed 29 July 2017)

CompleteDissertation (2019). "CompleteDissertation by Statistics Solutions Expert Guidance Every Step of the Way." https://www.statisticssolutions.com/correlation-pearson-kendall-spearman/. (accessed 9 March 2019).

Cooney, J. J. (1988). "Microbial transformations of tin and tin compounds." *J. Ind. Microbiol.*, 3(4):195–204.

de Smeth, J.B. (2005). Book chapter. "Environmental and Exploration Geochemistry." *Earth Resource Exploration*., Enschede, ITC: 39.

Easy Day Phuket. (2013). Phuket's Tin Mining Industry; http://www. easydayphuket.com/ blog/phukets-mining-history.

Edelstein, M., Ben-Hur, M. (2018). "Heavy metals and metalloids: Sources, risks and strategies to reduce their accumulation in horticultural crops." *Sci. Hortic-Amsterdam*., 234, 431-444.

Environmental Geophysics. (2016). "Resistivity methods." https://archive.epa.gov/esd/archivegeophysics/web/html/resistivity_methods.html (accessed 18 May 2016)

EPA, (1996). Method 3052. "Microwave assisted acid digestion of siliceous and organically based matrices." Available from: www.epa.gov/epaoswer/hazwaste/test/3052.pdf. (Accessed 3 February 2017)

Freije, A. M. (2015). "Heavy metal, trace element and petroleum hydrocarbon pollution in the Arabian." *J. Assoc. Arab Univ. Basic Appl. Sci.*, 17, 90-100.

Ganugapenta, S., J. Nadimikeri, Chinnapolla, S. R. R. B., Ballari, R. Madiga, N. K and Tella, L. P. (2018). "Assessment of heavy metal pollution from the sediment of Tupilipalem Coast, southeast coast of India." *INT. J. SEDIMENT. RES.*, 165. https://doi.org/10.1016/j.ijsrc.2018.02.004

Garson, M. S., Young, B., Mitchell, A. H. G., Tait, B. A. R., Bateson, J. H., Cogger, N., Johnson, R. L., Prewett, W. G., Stephens, E. A. (1975). "The Geology of the Tin Belt in Peninsular Thailand around Phuket, Phangnga, and Takua Pa." first ed. *HMSO*, London.

Gautam, S., Patra, A., Sahu, S. and Hitch, M. (2016). "Particulate matter pollution in opencast coal mining areas: a threat to human health and environment." *INT. J. MIN. RECLAM. ENV*., 32(2), 75–92. doi:10.1080/17480930.2016.1218110

Ghanbarpour, M. R., Goorzadi, M., Vahabzade, G. (2013). "Spatial variability of heavy metals in surficial sediments: Tajan River Watershed, Iran. Sustain." *Sustain. Water Qual. Ecol.*, 1-2, 48-58.

González-Acevedo, Z. I., García-Zarate, M. A., Núñez-Zarco, E. A., and Anda-Martín, B. I. (2018). "Heavy metal sources and anthropogenic enrichment in the environment around the Cerro Prieto Geothermal Field, Mexico." *Geothermics.*, 72: 170-181

Grellier, S., Gue´rin, R., Robain, H., Bobachev, A., Vermeersch, F., Tabbagh, A. (2004). "Monitoring of Leachate Recirculation in a Bbioreactor Landfill by 2-D Electrical Resistivity value Imaging." *J. ENVIRON. ENG. GEOPH.*, 1-10.

Guinea, A., Playà, E., Rivero, L., and Himi, M. (2010). "Electrical resistivity tomography and induced polarization techniques applied to the identification of gypsum rocks." *NEAR. SUF. GEOPHYS.*, 8(1730). doi:10.3997/1873-0604.2010009.

Harikrishnan, N., Chandrasekaran, A., Ravisankar, R., Alagarsamy, R. (2018). "Statistical assessment to magnetic susceptibility and heavy metal data for

characterizing the coastal sediment of the east coast of Tamilnadu, India." *Appl. Radiat. Isot*., 135, 177-183.

Helali, M. A., Oueslati, W., Zaaboub, N., Added, A., Aleya, L. (2016). "Bioavailability and assessment of heavy metal pollution in sediment cores off the Mejerda river delta (Gulf of Tunis): How useful is a multiproxy approach?" *Mar. Pollut. Bull.*, 105, 215-226.

Ilgar, R. and Sari, E. (2008). "Heavy Metals Distribution in Sediments from Dardanelles." *J. Appl. Sci*., 8(16), 2919-2923. doi:10.3923/jas.2008.2919.2923

Jolanta Pierwola. (2013). "Investigation of Soil Contamination Using Resistivity and Induced Polarization Methods." *Pol. J. Environ. Stud*., 22(6): 1781-1788.

Jones, F. (2007). "Geophysics foundations: Physical properties: Chargeability." *UBC Earth and Ocean Sciences.* Search Earth, Ocean and Atmospheric sciences. https://www.eoas.ubc.ca/ubcgif/iag/foundations/properties/2physprop-iag.htm (accessed 14th May 2018)

Kennish, M. J. (1996). "Practical handbook of estuarine and marine pollution.", in: Petralia, P., Carelli, C., Fortener. S., Jaffe, G. (Eds.), *Heavy Metals*. CRC Presistivity values., New York, pp. 253-298.

Kloke, A., Sauerbeck, D. R., Vetter, H. (1984). "The contamination of plants and soil with heavy metals and the transport of metals in terrestrial food chain." In: Nriagu JO, ed. *Changing metal cycles and human health*. Berlin, Springer-Verlag, pp. 113–141.

Koda, E., Tkaczyk, A., Lech, M., Osiński, P. (2017). "Application of Electrical Resistivity Data Sets for the Evaluation of the Pollution Concentration Level within Landfill Subsoil." *Appl. Sci*., 7(3), 262. doi:10.3390/app7030262

Kura, N. U., Ramli, M. F., Ibrahim, S., Sulaiman, W. N. A., Aris, A. Z. (2014). "An integrated assessment of seawater intrusion in a small tropical island using geophysical, geochemical, and geostatistical techniques." *Environ. Sci. Pollut. Res. Int*., 21-11, 7047–7064.

Kusin, F. M., Azani, N. N. M., Hasan, S. N. M. S., Sulong, N. A. (2018). "Distribution of heavy metals and metalloid in surface sediments of the heavily-mined area for bauxite ore in Pengerang, Malaysia and associated risk assessment." *Catena*., 165, 454-464

Lærd statistic. (2019). “Pearson Product-Moment Correlation.” https://statistics.laerd.com/statistical-guides/pearson-correlation-coefficient-statistical-guide.php (accessed 13 January 2019).

Léopold, E. N., Jung, M. C., Auguste, O., Ngatcha, N., Georges, E., Lape, M. (2009). “Metals pollution in freshly deposited sediments from river Mingoa, main tributary to the Municipal lake of Yaounde, Cameroon.” *Geosci. J.*, 12(4), 337-347. doi:10.1007/s12303-008-0034-5

Lverson, K., (2017). “The best Thai islands to visit to avoid tourists. Culture Trip.” https://theculturetrip.com/asia/thailand/articles/the-best-thai-islands-to-visit-to-avoid-tourists/ (accessed 18 January 2017).

Martinho, E., Almeida, F., Matias, M. J. S. (2004). “Time-domain induced polarization in the determination of the salt/freshwater interface (Aveiro - Portugal)”. *Cartagena.*, 2004.

Mathizhagan, M., Selvakumar, T., Ganesan, M. (2012). “Geophysical technique for sensing of solid waste dump site-induced groundwater contamination leachate.” *Poll. Res.*, 32(3), 509-514.

MathSteps. (2018). “What is it? Linear Equations.” https://www.eduplace.com/math/mathsteps/7/d/index.html. (accessed 25 October 2019)

Mohiuddin, K. M., Islam, M. S., Basak, S., Abdullah, H. M., Ahmed, I. (2016). “Status of heavy metal in sediments of the Turag river in Bangladesh.” *Progress. agric.*, 27(2). doi:10.3329/pa.v27i2.29315

Müller, G. (1981). “The heavy metal pollution of the sediments of Neckars and its tributary: a stocktaking.” *Chem. Ztg*., 105, 157e164

National Geogrphic. (2019). “Sediment. Education-Classroom Resources section.” https://www.nationalgeographic.org/encyclopedia/sediment/ (accessed 5 April 2019).

National Rivers Authority. (1994). “Abandoned mines the water environment, 1994.” http://www.environmentdata.org/archive/ealit:4107

National Statistical Office. (2017). “Ministry of Information and Communication Technology.” http://web.nso.go.th/

Neeti, K., Prakash, T. (2013). "Effects of heavy metal poisoning during pregnancy." *Int. Res. J. Eviron. Sci.*, 2(1), 88-92.

NRC. (2014). "MESS-4: Marine Sediment Reference Material for Trace Metals and Other Constituents." National Research Council of Canada. https://www.nrc-cnrc.gc.ca/eng/solutions/advisory/crm/certificates/mess_4.html/. (Accessed 2 January 2018).

Nurbaiti, U. (2011). "Magnetic properties of suspended of polluted heavy metal sediments from Semarang rivers." *Jurnal Pendidikan Fisika Indonesia*., 7(2011): 134-137.

Nzeve, J. K., Kitur, C. E., Njuguna, S. G. (2014). "Determination of Heavy Metals in Sediments of Masinga Reservoir, Kenya." *ENVIRON. EARTH. SCI.*, 4.

Organization, W.H. (2005). "Tin and Inorganic Tin Compounds." *Geneva*.

Plata, J. L., Rubio, F. M., (2004). "Study of the salt water - freshwater interface in environments of low resistivity: Donana Aquifer (Spain)." *Cartagena.*, 18 SWIM: 435-446.

Puttiwongrak, A., Suteerasak, T., Mai, P. K., Hashimoto, K., Gonzalez, J. C., Rattanakom, R., Prueksakorn, K. (2019). "Application of multi-monitoring methods to investigate the contamination levels and dispersion of Pb and Zn from tin mining in coastal sediments at Saphan Hin, Phuket, Thailand." *J. CLEAN. PROD.*, 218, 108-117. doi:10.1016/j.jclepro.2019.01.254

Rachwał, M., Kardel, K., Magiera, T., Bens, O. (2017). "Application of magnetic susceptibility in assessment of heavy metal contamination of Saxonian soil (Germany) caused by industrial dust deposition." *Geoderma*., 295, 10-21.

Rajeswari, T. R., Sailaja, N. (2014). "Impact of heavy metals on environmental pollution." *J. Chem. Pharm. Res.*, 3, 175-181.

Ravisankar, R., Harikrishnan, N., Chandrasekaran, A., Gandhi, M. S., Alagarsamy, R. (2017). "Data on heavy metal and magnetic relationships in coastal sediments from southeast coast of Tamilnadu, India." *Data In Brief*., 16 (2018), 392-400.

Rehman, F., Abuelnaga, H. S. O., Harbi, H. M., Cheema, T., Atef, A.H. (2016). "Using a combined electrical resistivity imaging and induced polarization techniques with the chemical analysis in determining of groundwater pollution

at Al Misk Lake, Eastern Jeddah, Saudi Arabia." *ARAB. J. GEOSCI.*, 9(4). doi:10.1007/s12517-016-2423-9

Remeikaite-Nikiene, N., Garnaga-Budre, G., Lujaniene, G., Joksas, K., Stankevicius, A., Malejevas, V., Bariseviciute, R. (2018). "Distribution of metals and extent of contamination in sediments from the south-eastern Baltic Sea (Lithuanian zone)." *Oceanologia.*, 60, 193e206.

Sakanann, V. (2018). **"**Preliminary Assessment of Seawater Intrusion in Phuket Island, Thailand." *Prince of Songkla University, Thailand* (Master Thesis).

Sakunboonpanich, Y. (2011). "History of the modern city of Phuket from 1957-2007." *University of Thammasat* (Master Thesis).

Salah, E. A. M., Zaidan, T. A. and Al-Rawi, A. S. (2012). "Assessment of Heavy Metals Pollution in the Sediments of Euphrates River, Iraq." *JWARP*., 04(12): 1009-1023.

Santschi, P. H., Hohener, P., Benoit, G., Bucholtz-ten, B.M. (1990). "Chemical processes at the sediment-water interface." *Mar. Chem.*, 30, 269–315.

Saraee, R. E. K., Abdi, M. R., Naghavi, K., Saion, E., Shafaei, M. A., Soltani, N. (2011). "Distribution of heavy metals in surface sediments from the South China Sea ecosystem, Malaysia." *Environ. Monit. Assess.*, 183(1-4), 545-54. doi:10.1007/s10661-011-1939-4

Satpathy, K. K., Mohanty, A. K., Prasad, M. V. R., Natesan, U., Sarkar, S. K. (2011). "Studies on the variations of heavy metals in the marine sediments off Kalpakkam, East Coast of India." *ENVIRON. EARTH. SCI.*, 65(1): 89-101.

Schober, P., Boer, C. and Schwarte, L. A. (2018). "Correlation Coefficients: Appropriate Use and Interpretation." *Anesth. Analg.*, 126(5): 1763-1768.

Sharifuzzaman, S. M., Rahman, H., Ashekuzzaman, S. M., Islam, M. M., Chowdhury, S. R., Hossain, M. S. (2016). Environmental remediation technologies for metal-contaminated soils in: *Heavy Metals Accumulation in Coastal Sediments*. Springer, Japan, pp. 21-42.

Sharma, P. V. (1997). *Environmental and engineering geophysics*. Cambridge University Presistivity values, Cambridge.

Siripong. (2013). “The History of Phuket’s Tin Mine Industry.” https://live.phuketindex.com/the-history-of-Phuket's-tin-mining-industry-2093.html (accessed 16 March 2015)

Soralump, S. (2010). “Corporative of Geotechnical Approach for Landslide Susceptibility Mapping in Thailand. In: International Conference on Slope 2010.” Geotechinique and Geosynthetics for Slope, Chiangmai, Thailand.

Srigutomo, W.,Trimadona and Pratomo, P. M. (2016). “2D Resistivity and Induced Polarization Measurement for Manganese Ore Exploration.” *Journal of Physics: Conference Series., 739*, 012138. doi:10.1088/1742-6596/739/1/012138

Statistics How To. (2019). “Correlation Coefficient: Simple Definition, Formula.” *Easy Steps*. https://www.statisticshowto.datasciencecentral.com/probability-and-statistics/correlation-coefficient-formula/ (accessed 09 April 2019)

Suteerasak, T., Akkajit, P. (2018). “Using the Grain size and concentration of Pb and Zn in sediments to identify the layer of sediment from tsunami in 2547 B.E. (2004 C.E.) in the Bang Yai estuary, Phuket Bay.*” J. Sci. Technol.,* 26 (3), 459-475 (in Thai).

Suteerasak, T., Bhongsuwan, T. (2006). “Concentration of heavy metal As, Pb, Mn, Ni, Sn, Zn, Cr, Fe, and radon gas in bottom sediment from abandoned tin mines in the Phuket Province.” *J. Sci. Technol.,* 28 (3), 641-654 (in Thai).

Suteerasak, T., Bhongsuwan, T. (2008). “Contamination of heavy metals Al, As, Cu, Cr, Mn, Ni, Pb, Sn, Zn and Fe in sediment from Bang-Yai River in Phuket province.*” J. Res. Development.,* 31 (4), 765-779 (in Thai).

Temara, A., Skei, J. M., Gillan, D., Warnau, M., Jangoux, M., Dubois, P. (1998). “Validation of the asteroid Asterias Rubens (Echinodermata) as a bioindicator of spatial and temporal trends of Pb, Cd, and Zn contamination in the field.” *Mar. Environ. Res*., 45, 341–356.

Uchegbulam, O., Ayolabi, E. A. (2014). “Application of electrical resistivity imaging in investigating groundwater pollution in Saplele area, Nigeria.” *JWARP*., 6, 1369-1379.

US Environmental Protection Agency (USEPA). (1996). *Acid digestion of sediments, sludges, and soils*. Methods 3050B.

Ustra, A. T., Elis, V. R., Mondelli, G., Zuquette, L. V. and Giacheti, H. L. (2011). "Case study: a 3D resistivity value and induced polarization imaging from downstream a waste disposal site in Brazil." *ENVIRON. EARTH. SCI.*, 66(3), 763-772. doi:10.1007/s12665-011-1284-5

Wafi, H.N. (2015). "Assessment of Heavy Metals Contamination in the Mediterranean Sea along Gaza Coast - A Case Study of Gaza Fishing Harbor." *Al-Azhar University-Gaza* (Master Thesis).

Weesakul, U., and Lowanichchai, S. (2005). "Rainfall forecast for agricultural water allocation planning in Thailand. Thammasat Int." *Journal of Science Technology*., 10 (3), 18-27.

Wu, J., Lu, J., Li, L., Min, X., Luo, Y. (2018). "Pollution, ecological-health risks, and sources of heavy metals in soil of the northeastern Qinghai-Tibet Plateau." *Chemosphere.*, 201, 234-242.

Xiang-bin, S., Gui-xiang, L., Xiang-jing, F., Jin-ping, S., Liping, H., Bo, B. (2015). "Heavy Metal Contents and Accumulation Characteristic of Dominant Plants in Tin Mining Wasteland of Gejiu city, Yunnan, China." In: 5th International Conference on *Advanced Design and Manufacturing Engineering*, *Atlantis Presistivity values*, China, pp. 801-808.

Yaacob, W. Z. W., PauZi, N.S.M., Mutalib, H.A. (2009). "Acid mine drainage and heavy metals contamination at abandoned and active mine sites in Pahang." *Bulletin of the Geological Society of Malaysia.*, 55(2009), 15-20.

Younis, M. H. Y., Tesfamariam, Z. (2017). "Geochemical analysis of sediment samples from Asmara drinking water reservoirs for estimation of contamination by heavy metals (IV)." *Am. J. Res. Commun.*, 5(1), 65-79.

VITAE

Name Phuong Khanh Mai

Student ID 6030420005

Educational Attainment

Degree	Name of Institute	Year of Graduation
Master of Science (Earth System Science)	Prince of Songkla University Phuket Campus	2019

Scholarship and Awards during Enrolment

2017 - 2019 Thailand's Education Hub (TEH-AC), from 2017 to 2019

2018 - 2019 The fifteenth regional congress on Geology, Mineral and Energy resources of Southeast ASIA (GEOSEA XV) at Hanoi, Vietnam
Topic: Application of Integrated Business Intelligence Model and Landslide Modeling for Data Management and Visualization of Historical Landslides: A case study of Patong Landslide, Phuket Island

List of Publications

Avirut Puttiwongrak, Thongchai Suteerasak, **Phuong Khanh Mai**, Kiyota Hashimoto, Jorge Carlos Gonzalez, Rawee Rattanakom, Kritana Prueksakorn, 2019. Application of multi-monitoring methods to investigate the contamination levels and dispersion of heavy metals from tin mining in coastal sediments at Saphan Hin, Phuket, Thailand. Journal of Cleaner Production. 218 (2019). 108-117.